applied sciences

MDPI

Article

Developing a Library of Shear Walls Database and the Neural Network Based Predictive Meta-Model

Mohammad Javad Moradi [1] and Mohammad Amin Hariri-Ardebili [2,*]

[1] Department of Civil Engineering, Razi University, Kermanshah 67144-14971, Iran; javad_moradi1988@yahoo.com

[2] Department of Civil Environmental and Architectural Engineering, University of Colorado, Boulder, CO 80302, USA

* Correspondence: mohammad.haririardebili@colorado.edu; Tel.: +1-303-990-2451

Received: 26 May 2019; Accepted: 19 June 2019; Published: 23 June 2019

Abstract: There is a large amount of useful information from past experimental tests, which are usually ignored in test-setup for the new ones. Variation of assumptions, materials, test procedures, and test objectives make it difficult to choose the right model for validation of the numerical models. Results from different experiments are sometimes in conflict with each other, or have minimum correlation. Furthermore, not all these information are easily accessible for researchers and engineers. Therefore, this paper presents the results of a comprehensive study on different experimental models for steel plate and reinforced concrete shear walls. A unique library of up to 13 parameters (mechanical properties and geometric characteristics) affecting the strength, stiffness and drift ratio of the shear walls are gathered including their sensitivity analysis. Next, a predictive meta-model is developed based on artificial neural network. It is capable of forecasting the responses for any desired shear wall with good accuracy. The proposed network can be used to as an alternative to the nonlinear numerical simulations or expensive experimental test.

Keywords: steel plate shear wall; reinforced concrete shear wall; meta-model; neural network

1. Introduction

Bertero [1] defined the shear wall (SW) as a very stiff member, with high resistance to deformation under load. *"It is essentially a plate loaded in its own plane, but the analysis needed to predict its behavior is more complicated than that of simple plates"* [1]. Shear walls resist lateral forces parallel to their plane. The slender walls (where the bending deformation is of concern) resist the loads due to cantilever action. In general, the SW system can be classified as reinforced concrete shear walls (RCSW) [2–4], steel plate shear wall (SPSW) [5,6], masonry shear walls [7–9], composite shear walls, and timber plate shear walls [10,11]. Although the RCSWs have longer history than SPSWs in structural engineering (due to their remarkable strength and lateral stiffness), the application of SPSWs has also increased in the past few decades [12,13]. SPSWs reduce the overall steel consumption, they are lighter compared to other walls, and they can be easily adopted in existing or damaged buildings [14,15]. SPSWs were also added to the design codes as an acceptable lateral load bearing systems [16,17].

The proper design of a SW can provide energy absorption, stiffness, ductility, and appropriate behavior under cyclic/seismic loading. The adequate stiffness of the lateral load bearing system may reduce the story drift and fulfill the code requirements. Quantification of the strength, stiffness and ductility leads to a precise performance evaluation of the SW systems.

Design and/or analysis of a SW system requires proper background information about the mechanism and performance of these systems. Often, the numerical models should be validated based on the experimental tests [18]. There is a very large set of SW experiments tested by different

researchers with various assumptions and purposes. The results are sometimes in conflict with each other or at least have minimum correlation. This makes the model selection quite difficult. In addition, not all these information are easy to collect and process by engineers (as they might be copyrighted or restricted materials). The authors have been confronted by such a problems in their previous studies on both steel and RC shear walls from experimental [15] and numerical [19] points of view. This was one of the motivations to develop such a comprehensive database of SW models, which would be useful for all the future studies related to the experimental and numerical validations.

On the other hand, such a huge database might be difficult to track by practitioners, and, thus, a meta-model is required to summarize and present the results in a systematic way. This should include the parameters affecting the stiffness and strength of the SWs, as well as their sensitivity. There exist many soft computing (or surrogate) techniques with different levels of sophistication that can be used to post-process a database [20]: artificial neural network (ANN), support vector machine [21], polynomial chaos expansion [22], etc. In this research, the ANN is selected, which has been proven to be one of the best soft computing techniques, in nearly all engineering fields. The neural network can predict several outputs by receiving a set of input parameters. To do this, a neural network should be trained efficiently. Then, it can predict other results that have not been investigated before.

2. Research Significance and Contributions

The research significance can relay on the profuse investigation of the existing database of the SWs, as well as to provide a useful tool to fellow researchers. It is important to notice that the difficulty in obtaining large scale results for SWs behavior has greatly limited the research in the past for this important issue. This paper is intended to adopt one of the widely-used and well-established soft computing techniques (i.e., ANN) to solve an engineering problem. Comparing and contrasting various surrogate models are not the focus of this paper. The developed predictive meta-model can be used as a useful alternative in the absence of detailed experiments or numerical simulations. The contribution of the authors in this paper can be summarized as follows:

- Developing a large library of SW experimental tests for both the steel plate and reinforced concrete materials
- Training and developing an ANN-based meta-model for SWs for response prediction purposes
- Providing an active library of data which can be easily updated by any new information
- Performing sensitivity analysis of the responses to the input parameters
- Proposing a predictive models for stiffness and strength for both types of SWs, as well as the drift ratio for RCSWs

The paper starts with a brief description on ANN model and its fundamental features in Section 3 (for those readers who are not familiar with this concept). Next, the comprehensive database is introduced in Section 4. The ANN training process and meta-models are then presented in Section 5 followed by the sensitivity analysis. Finally, Section 6 provides the general conclusions and recommendations. Detailed information about the SW library, and the developed neural network model can be found in Appendixes A and B, respectively.

3. Artificial Neural Network

An ANN is inspired by the human brain, in which the neurons are tasked with data processing. By gathering these neurons, the layer is produced, and an ANN may consist of several layers. Neurons are connected by weighted synapse. Finally, the input data exit from the output layer after applying numerical processing on them [23,24]. Hebb [25], Widrow and Hoff [26] and Rosenblatt [27] offered fundamentals and extensions of the ANN. Research on the neural network continued until 1985, and Rumelhart et al. [28] proposed multi-layer perceptron (MLP) with back-propagation algorithm. Subsequently, various models and networks were presented and research is still ongoing [29].

A MLP is a type of neural network in which neurons are deployed on more than one layer. An output of nth neuron in the mth layer in a generic MLP is determined as:

$$O_n^m = f_n^m \left(\left(w^{(m-1)} \right)^T O_n^{m-1} + b^m \right) \quad (1)$$

where f_n^m is the function of nth neuron in the mth layer, $w^{(m-1)}$ is the weights from $(m-1)$th to mth layer, and b^m is mth layer's bias term.

For the last layer, $n = 1$ and $O_n^m = \hat{y}$. The objective function for learning process is defined in a way to minimize the mean squared error (MSE $= \frac{1}{2N} \sum (y - \hat{y})^2$) between the observed value, y, and the estimated one, $\hat{y}$. This is an iterative procedure by initializing w value, estimating $\hat{y}$, and computing the corresponding MSE. If the obtained MSE falls outside the satisfactory range, the initial w should be updated.

The MLP is capable of classification, clustering, and function approximation. With a neural network of three [30–33] and four [34] layers, and sufficient number of neurons in the hidden layers, nearly any function can be estimated [23,35]. Usually, a four-layer network requires fewer weights to estimate the functions; however, it introduces more local minima [36].

The ANN is one of popular soft computing techniques in structural engineering and mechanics. Although there is much research and development, on both the theoretical aspects and application, some of the most relevant ones are reviewed in this section. Adeli and Seon Park [37] evaluated the maximum moment of a beam. Xu et al. [38] proposed a method for crack detection in plates using a MLP. De Lima et al. [39] evaluated three types of steel beam-column joints. It was observed that the neural network can properly estimate the bending strength of the connection; however, due to differences in the measurement systems, the network had extra error in estimation of the stiffness parameter. Abdalla et al. [40] provided an estimate of the shear strength of RC rectangular beams by examining the parameters such as concrete strength, reinforcement ratio, thickness, length, and width of the beam. It was observed that the network can estimate the shear strength of concrete beam with acceptable accuracy. More than 96% of the estimated neural network data had absolute error less than 15%, while it was 26% and 23% for UK and US standards estimated data, respectively. Kumar et al. [41] evaluated composite shell vibration. It was found that the response from the neural network for all of the loading patterns in the research was nearly identical to the response.

González and Zapico [42] determined the seismic failure in structures. The network inputs were the natural frequency of the structure and shape of the mode, and the output was mass and stiffness. The data were obtained using finite element analysis. The network showed a good performance in prediction of the structural behavior. Yan et al. [43] reviewed the structural failure of the beams using back propagation algorithm. It was observed that the neural network properly predicts the failure of the beams. Lee and Lee [44] predicted the shear strength of the RC beam reinforced with FRP by evaluating 106 experimental data using ANN. It was observed that the network can estimate shear strength with better accuracy than other available equations. Asteris and Plevris [45] proposed the application of ANNs to approximate the failure surface of the anisotropic masonry materials in a dimensionless form. They compared the derived results with experimental findings and analytical solutions, and reported a reliable performance for the ANN-based approximation of the masonry failure surface under biaxial stress. Toghroli et al. [46] reviewed various numerical methods to examine the parameters affecting the bearing capacity of composite beams. It was observed that extreme learning machine has the best result in estimating the composite beam behavior among other investigated methods. Naderpour et al. [47] proposed a method in which the geometric and mechanical properties of cross-section and FRP bars, and shear span-depth ratio were considered for concrete beams. The error in the shear strength estimation was about 9.7%, which was significantly lower than other methods and relationships.

Rezaei Rad and Banazadeh [48] presented a comprehensive application of probabilistic soft computing technique in damage determination of steel structure. Ghorbani et al. [49] used the MLP and radial basis function ANNs to predict the support pressure, and develop the ground motion curve in an underground structure (circular tunnel). An elastoplastic, strain-softening rock mass

was considered including both single- and double-layer hidden neurons. Asteris and Kolovos [50] proposed the application of ANNs to predict the mechanical characteristics of self-compacting concrete. The 28-day compressive strength of admixture-based self-compacting concrete was predicted, and a formula was proposed for the data normalization. Chen et al. [51] developed two hybrid surrogate models by combining ANN with imperialist competitive algorithm (ICA) and genetic algorithm. These techniques were used to predict the safety factor of retaining walls in dynamic condition. A very large database of 8000 designs were used for this purpose. They found that the ICA-ANN provides a better performance. Finally, Asteris and Nikoo [52] optimized the connection weights of the feed-forward ANNs using the artificial bee colony (ABC). The algorithm was then used to determine the fundamental period of reinforced concrete infilled structures. They confirmed the superior performance of this hybrid method over the traditional ones.

4. Library of Shear Wall Database

As stated in Section 1, a comprehensive library of SW databases is collected. It includes about 300 samples with 12 features for SPSWs, and about 4000 samples with 13 features for the RCSWs. Those features are listed in Tables 1 and 2. It should be noted that the SPSW models are without stiffener, slip, and opening and are non-corrugated.

Table 1. Statistics of the parameters in SPSW model.

Parameter	Symbol	Unit	Min	Max	Mean	STD
Frame Height	h_f	mm	500	1830	1073	283
Frame Width	b_f	mm	500	3660	1747.8	712.2
Column Area	A_c	mm^2	1070	18190	7598.5	4424.9
Column Moment of Inertia	I_c	mm^4	864,000	3.47×10^8	7.00×10^7	8.70×10^7
Beam Area	A_b	mm^2	1070	16,300	6163.1	3682
Beam Moment of Inertia	I_b	mm^4	864,000	6.37×10^8	6.10×10^7	1.20×10^8
Plate Height	h_p	mm	380	1500	1034	318.3
Plate Width	b_p	mm	380	3337	1360.8	668.8
Plate Thickness	t_p	mm	0.5	15	3.79	3.12
Plate Yield Stress	F_{yp}	Pa	295,000	4.20×10^8	2.50×10^8	1.00×10^8
Plate Ultimate Stress	F_{up}	Pa	2.60×10^8	5.60×10^8	4.10×10^8	9.60×10^7
Plate Modulus of Elasticity	E_p	Pa	1.50×10^{11}	2.00×10^{11}	1.80×10^{11}	2.20×10^{10}
Load Bearing Capacity	P	N	11,480	3,020,000	1,056,303	795,832
Lateral Stiffness	K	N/mm	2380	181,000	68,983.2	45,897

Table 2. Statistics of the parameters in RCSW model.

Parameter	Symbol	Unit	Min	Max	Mean	STD
Axial Load	$A.L$	kN	0	3192	323	514.1
Boundary Element Length	W_{1b}	mm	0	380	123.6	99.6
Boundary Element Width	W_{2b}	mm	0	610	142.7	129
Vertical Column Reinforcement Ratio	ρ_{vc}	%	0	14.33	2.3	2.62
Horizontal Column Reinforcement Ratio	ρ_{ch}	%	0	6.69	0.75	0.93
Yield Stress of Column Reinforcement	F_{yc}	MPa	276	1412	495.6	181.6
Wall Height	h_w	mm	476	11,760	1812.5	1210.3
Wall Width	l_w	mm	450	5400	1389.2	685.2
Wall Thickness	t_w	mm	45	240	115	47
Vertical Wall Reinforcement Ratio	ρ_{vw}	%	0	14.33	0.74	1.47
Horizontal Wall Reinforcement Ratio	ρ_{hw}	%	0	6.69	0.47	0.54
Yield Stress of Wall Reinforcement	F_{yw}	MPa	216	1412	503.2	190.2
Concrete Compressive Strength	f'_c	MPa	9.5	93.6	35.3	14.6
Lateral Load Bearing	P	kN	15.42	3230.7	530.2	500
Lateral Stiffness	K	kN/mm	3.29	2933.7	209	341.8
Drift Ratio	D	%	0.21	6.9	1.65	1.05

Figure 1 illustrates the dimensions used for a generic SPSW and RCSW. Tables A1 and A2 (see Appendix A) illustrate the detailed library of SW database for steel plate and reinforced concrete walls, respectively. Feature selection should be included in all the aspects of the problem. The input parameters are in a wide range of variations, and should be normalized before using in the meta-model. Therefore, the data were linearly normalized in range of [0, 1]. This linear transformation preserves all the relationships of the initial database [53]. Initial weights were selected randomly focusing on the range of [−0.77, +0.77]. It has been empirically observed that this weight initialization technique leads to better performance and faster training of the ANN [54].

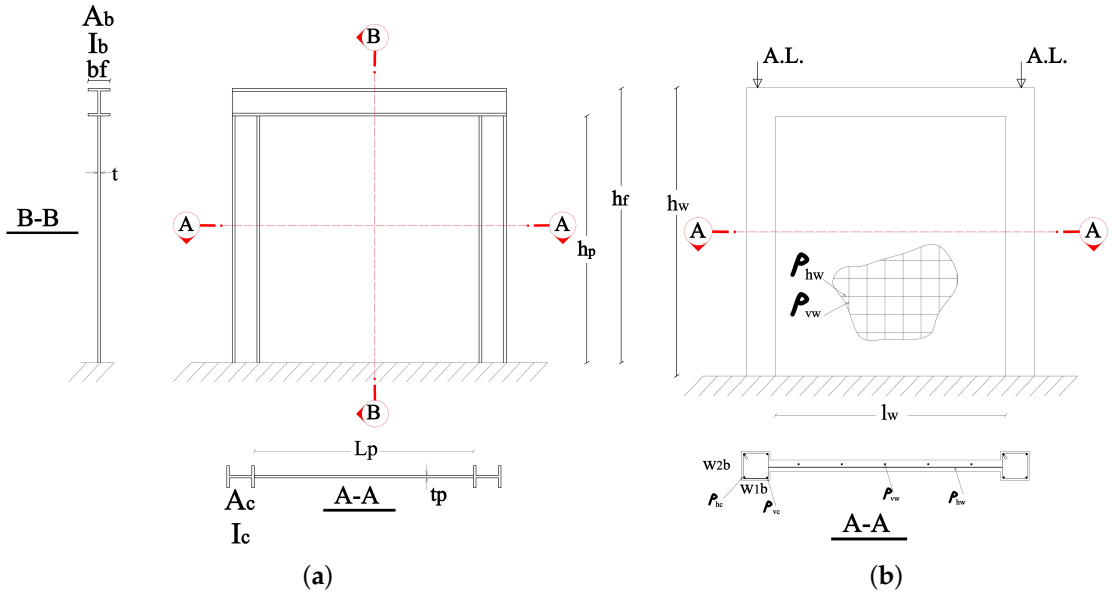

Figure 1. Dimensions of a generic shear wall. (**a**) SPSW, (**b**) RCSW.

A poor weight initialization may cause divergence of the outputs or becoming stuck at the local minima [23]. Tables 1 and 2 show the statistics of the selected features for SPSWs and RCSWs, respectively. The target data were considered to be the maximum strength, *P*, and stiffness, *K*, for SPSWs, plus drift ratio, *D*, (in addition to *K* and *P*) for RCSWs. The choice of these parameters was based on the abundance of data (e.g., crack pattern) in the literature, as well as the proper SW behavior expression. By estimating these parameters, the geometric characteristics and the mechanical properties required to obtain the desired shear strength, stiffness and drift ratio can be determined (accounting for an appropriate reliability coefficient). In design of SPSWs, it is assumed that the boundary elements do not yield, thus the mechanical properties of these members are not included as a network input. In all experiments, the buckling and the collapse of the infill plate occurred prior to the boundary elements. The network is applicable to the initial design of the SWs, as well as to retrofit the existing ones.

5. Modeling the Network

5.1. Number of Neurons

When the desired performance of the network is accomplished, the learning process ends. On the other hand, the number of optimal neurons required for each layer is not known beforehand, and it is usually determined by trial and error. The constructive approach is used to overcome this problem. This method finds the smallest network that can provide the required performance, and is suitable for passing local responses (or local minima); however, it is time consuming [55]. Empirical research has been performed to determine the optimal number of neurons [56]. A summary of this research is presented in Table 3. The results of this table can be used to determine the range of changes in the

number of the optimal neurons, and also is a limit for the interval of trial and error. As can be seen, the number of neuron in the hidden layer range from 2 to 39. The network's MSE value is computed for each number of neurons in the hidden layer, while other parameters are kept constant.

Table 3. A survey on number of the hidden neurons.

Reference	Criteria for Neuron of Hidden Layer	SPSW	RCSW
Hecht-Nielsen [57]	$\leq 2N_i$	$\leq$24	$\leq$26
Hush [58]	$3N_i$	36	39
Ripley [59]	$\frac{N_i+N_o}{2}$	6.5	7
Gallant and Gallant [60]	$2N_i$	24	26
Wang [61]	$\frac{2N_i}{3}$	8	8.6
Masters [62]	$\sqrt{N_i+N_o}$	3.6	3.7
Paola [63]	$\frac{N_oN_i+0.5N_o\times(N_o^2+N_i)-1}{N_o+N_i}$	1.3	1.35
Li et al. [64]	$\left(\frac{\sqrt{8N_i+1}}{2}\right)-2$	2.9	3.1
Tamura and Tateishi [65]	N_i+1	13	14
Lai and Serra [66]	N_i	12	13
Nagendra [67]	N_i+N_o	13	14
Gencay [68]	$\ln(N_i)$	2.4	2.5
Chris Wong et al. [69]	$\frac{N_i+N_o}{2}$	6.5	7
Heaton [70]	$\frac{2N_i}{3}+N_o$	9	9.6
Zhang et al. [71]	$\frac{2^{N_i}}{N}+1$	14.6	3
Huang [72]	$\sqrt{(N_o+2)N_i}+2\sqrt{\frac{N_i}{(N_o+2)}}$	10	10.4
Ke and Liu [73]	$N_i+\sqrt{N}$	29	76
Trenn [74]	$\frac{(N_i+N_o+1)}{2}$	6	6.5
Shibata and Ikeda [75]	$\sqrt{N_oN_i}$	3.4	3.6
Hunter et al. [76]	N_i+1	13	14
Sheela and Deepa [77]	$\frac{4N_i^2+3}{N_i^2-8}$	4.2	4.2

Figure 2 shows the performance of the network based on MSE for train and test data as a function of number of neurons. Each ANN model (with particular number of neurons) was iterated 10 times and its mean was used to increase the accuracy of the model. The mean errors for each neuron is also summarized in Table 4. The best performance among the train and test data for SPSW belonged to the network with 6 neurons, i.e., ANN 12-6-1, where the first, second and third digits are the number of input nodes, hidden neurons, and output nodes, respectively. On the other hand, ANN 13-10-1 had the best performance for RCSW.

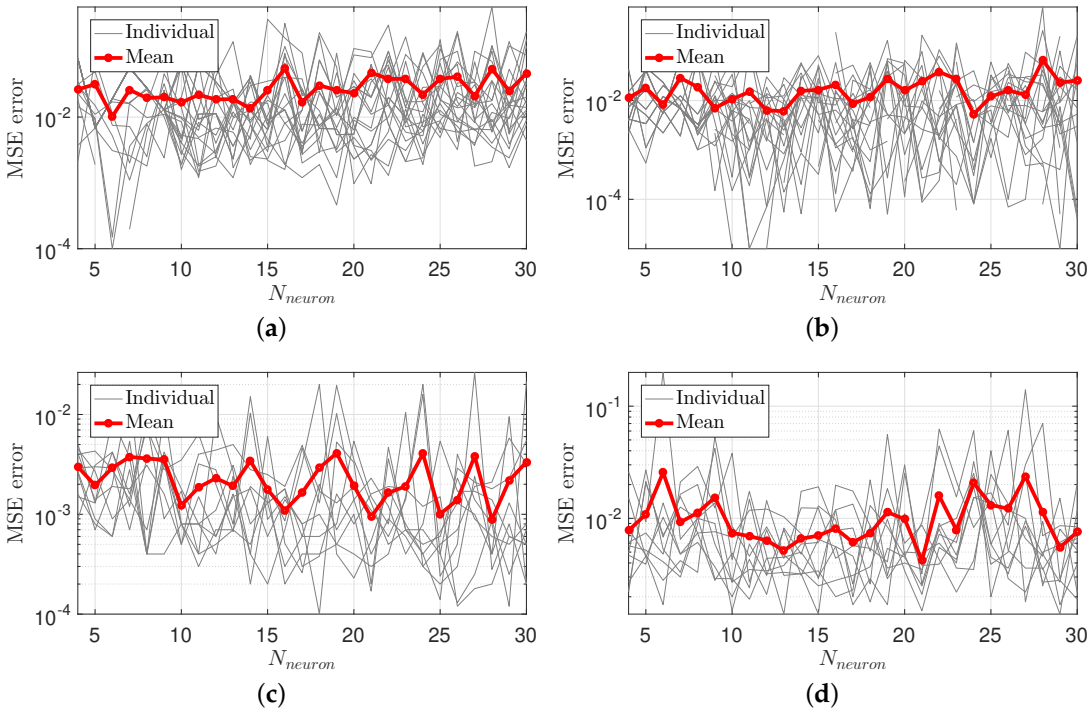

Figure 2. The network's neuron-dependent MSE. (**a**) SPSW; train data, (**b**) SPSW; test data, (**c**) RCSW; train data, (**d**) RCSW; test data.

Table 4. Mean MSE for train and test data as a function of number of neurons.

Neurons	SPWS		RCSW	
	Train Data	Test Data	Train Data	Test Data
4	0.0262	0.0113	0.0029	0.0078
5	0.0316	0.0180	0.0019	0.0109
6	0.0102	0.0082	0.0029	0.0257
7	0.0259	0.0285	0.0038	0.0092
8	0.0195	0.0187	0.0036	0.0112
9	0.0200	0.0070	0.0035	0.0153
10	0.0167	0.0107	0.0012	0.0074
11	0.0217	0.0149	0.0023	0.0069
12	0.0185	0.0063	0.0019	0.0064
13	0.0188	0.0061	0.0034	0.0052
14	0.0135	0.0156	0.0018	0.0066
15	0.0253	0.0164	0.0011	0.0070
16	0.0545	0.0208	0.0016	0.0081
17	0.0169	0.0087	0.0029	0.0061
18	0.0303	0.0117	0.0041	0.0074
19	0.0256	0.0273	0.0019	0.0113
20	0.0230	0.0159	0.0009	0.0099
21	0.0473	0.0242	0.0016	0.0042
22	0.0380	0.0380	0.0019	0.0159
23	0.0380	0.0270	0.0041	0.0079
24	0.0220	0.0053	0.0010	0.0206
25	0.0380	0.0120	0.0014	0.0132
26	0.0410	0.0160	0.0038	0.0122
27	0.0210	0.0130	0.0009	0.0237
28	0.0535	0.0648	0.0022	0.0113
29	0.0251	0.0229	0.0033	0.0055
30	0.0459	0.0254	0.0019	0.0076

5.2. Performance of the Network

Once the network is trained, it can be used to define the complex relationship among the input parameters, and to predict the output for any new SW model. Generalization means estimating the value on the hyper-surface where there are no available data. Mathematically, the learning process is a nonlinear curve-fitting algorithm, while generalization is the interpolation and extrapolation of the input data [47]. The ability of a network to generate new outputs depends on the number of parameters involved in the problem, the complexity of the parameters, and the structure of the network.

The neural network is constructed based on the number of neurons obtained from previous section. Figure 3 shows the architecture of the proposed networks for both SWs. In this paper, two MLPs are used to estimate the load bearing capacity, stiffness, and drift ratio of the SPSWs and RCSWs.

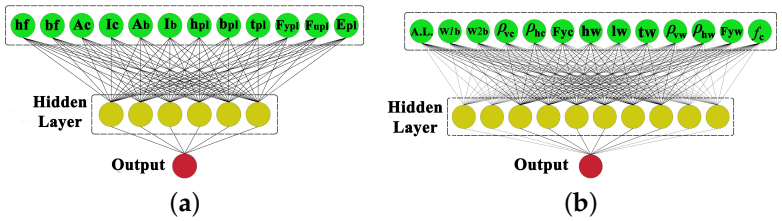

Figure 3. Proposed ANN models for shear walls. (**a**) SPSW, (**b**) RCSW.

Overall, 70% of data were used for training, 15% for validation, and 15% for testing. The validation and test data monitor the network over-training and performance, respectively. Performance of the network is shown in Figure 4. It states that the network has specific MSE for *n*th epoch, and there is no un-convergence or over-fitting.

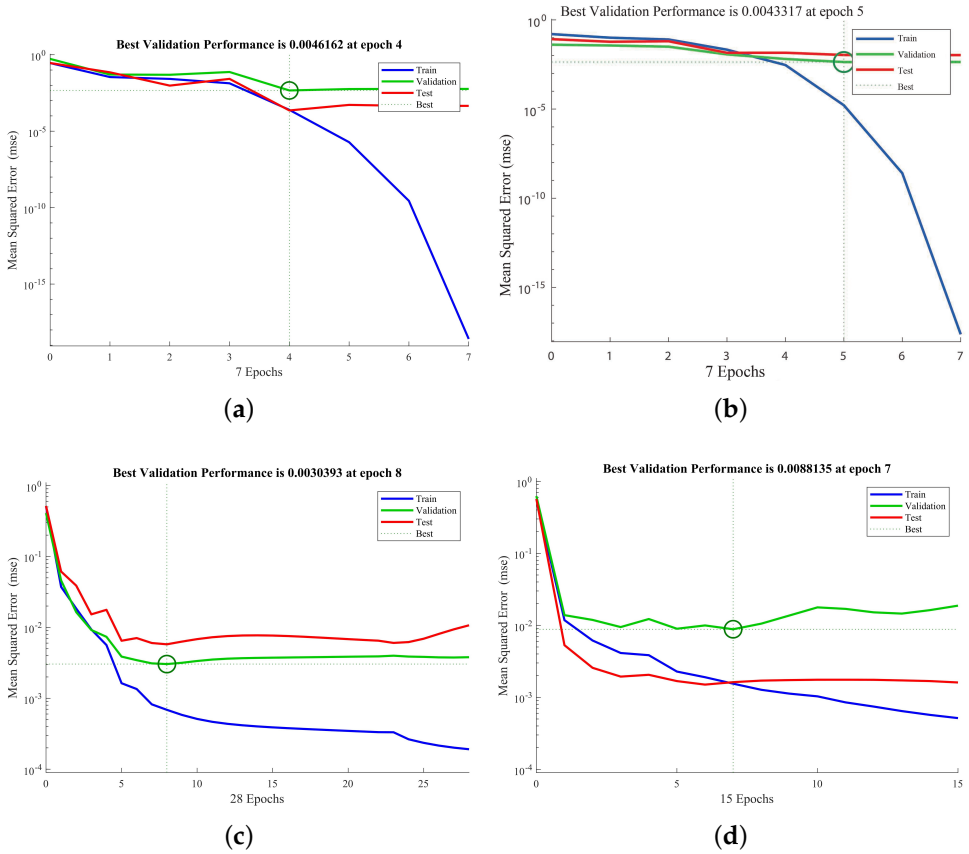

Figure 4. *Cont.*

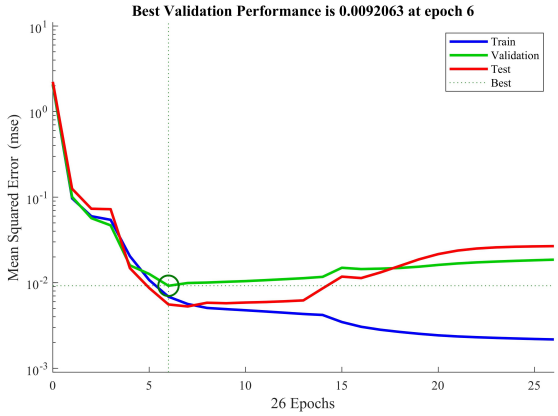

(**e**)

Figure 4. Performance function of the proposed network. (**a**) SPSW; Stiffness, (**b**) SPSW; Strength, (**c**) RCSW; Strength, (**d**) RCSW; Stiffness, (**e**) RCSW; Drift.

Furthermore, Figure 5 illustrates the quality of the estimation as a function of coefficient of determination, R2, in both SPSW and RCSW models. Finally, the MSE values for these data are summarized in Table 5. The proper performance of the network is evident in the estimation of the strength, stiffness and drift ratio of SWs. Therefore, the proposed network can learn the relation between the input and output parameters, and provide the results with appropriate accuracy. Finally, the true values of the strength, stiffness and drift ratio from experimental data and the predictive ANN-based meta-model are compared in Figure 6.

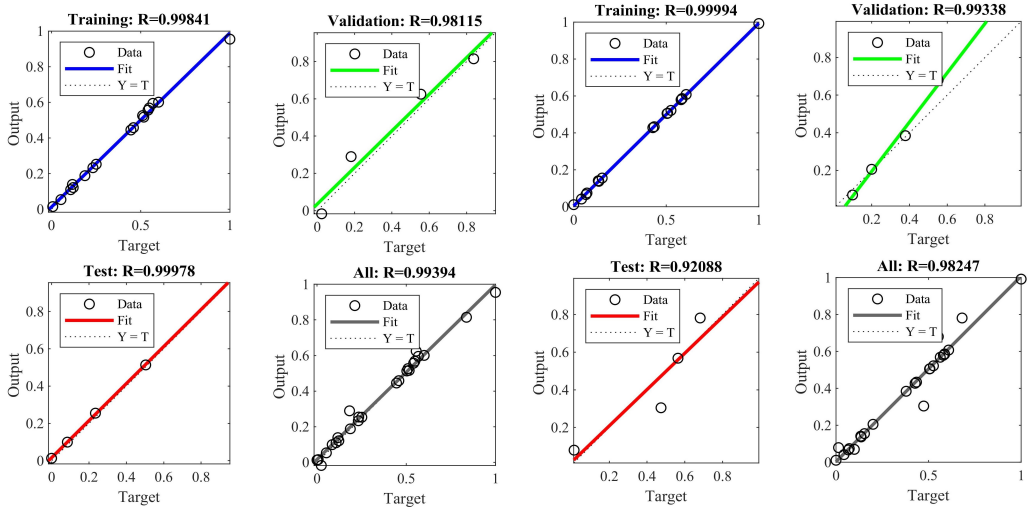

(**a**) (**b**)

Figure 5. *Cont.*

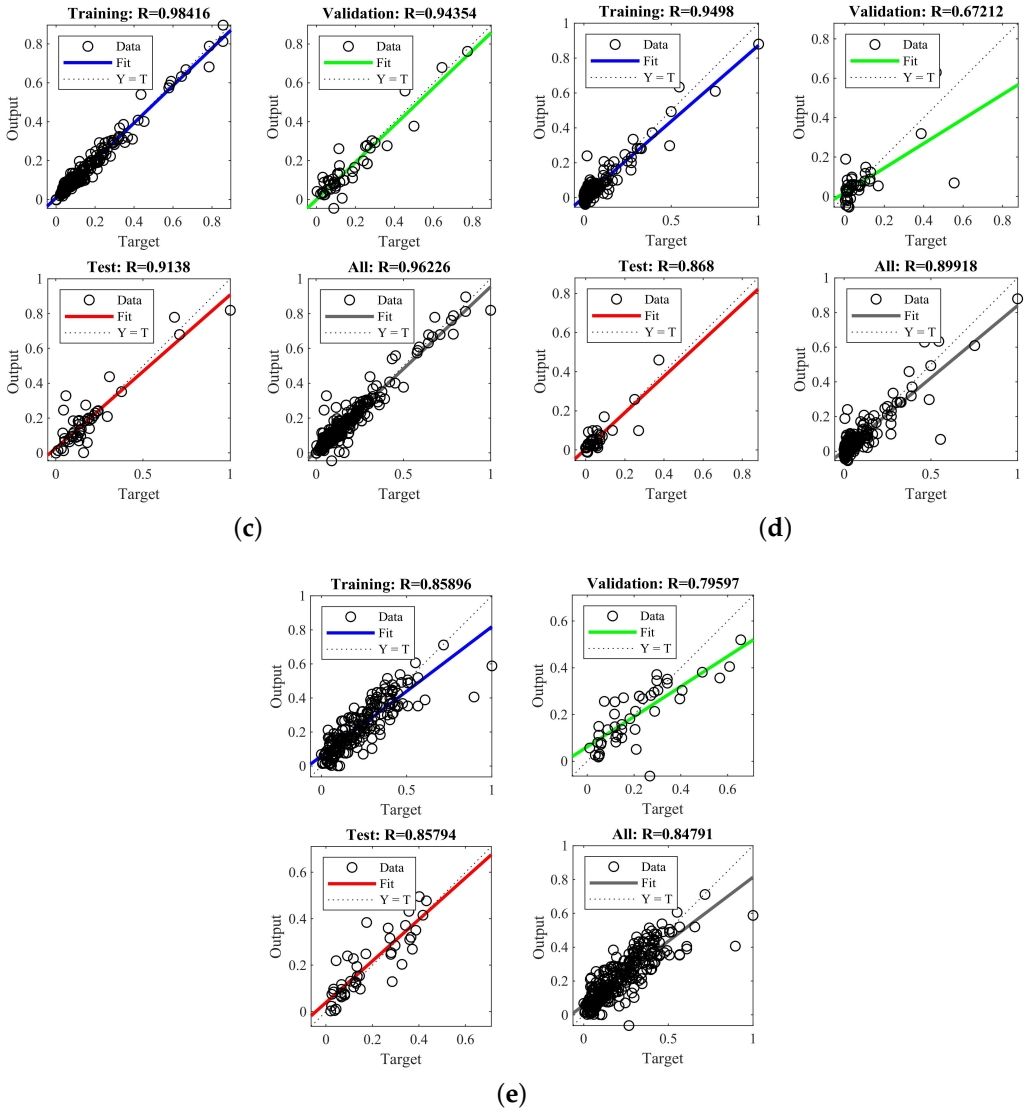

Figure 5. Regression values for the proposed ANN meta-model. (**a**) SPSW; Strength, (**b**) SPSW; Stiffness, (**c**) RCSW; Strength, (**d**) RCSW; Stiffness, (**e**) RCSW; Drift ratio.

Table 5. MSE values for training, validation and test data.

Output	Train	Validation	Test
Strength of SPSW	2.49×10^{-4}	0.0046	2.28×10^{-4}
Stiffness of SPSW	1.64×10^{-5}	0.0043	0.0108
Strength of RCSW	0.00743	0.0034	0.00123
Stiffness of RCSW	6.45×10^{-4}	0.0038	0.0061
Drift ratio of RCSW	0.0069	0.0059	0.0056

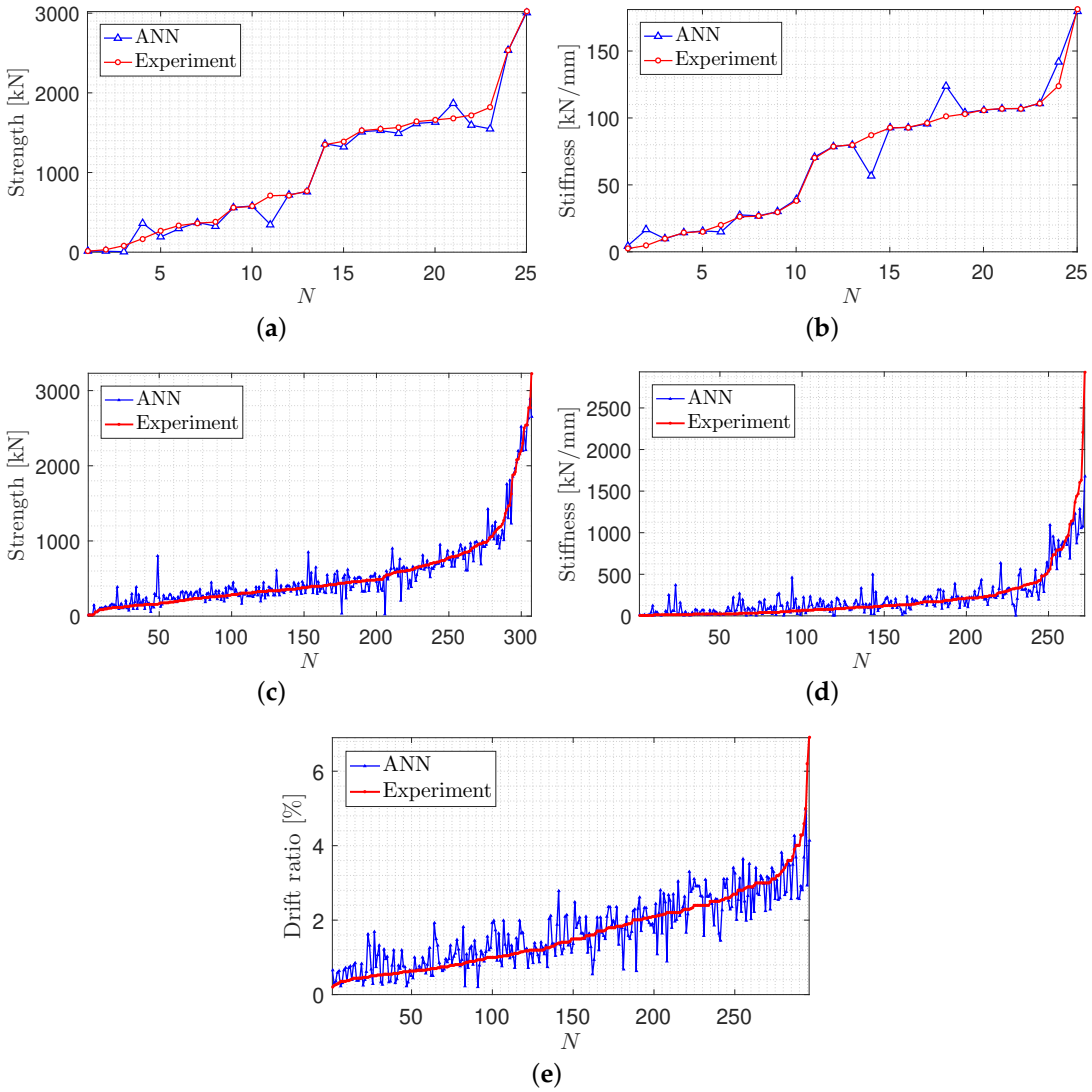

Figure 6. Comparison of measured experiments and predicted ANN meta-model; Note: sorted in ascending order based on experimental data. (**a**) SPSW; Strength, (**b**) SPSW; Stiffness, (**c**) RCSW; Strength, (**d**) RCSW; Stiffness, (**e**) RCSW; Drift.

Thus far, a detailed performance is discussed with respect to MSE. However, one may evaluate the predictive meta-models using other statistical indicators such as root mean square error (RMSE), Nash–Sutcliffe efficiency (NSE) coefficient, mean absolute error (MAE), and correlation coefficient (R). These metrics can be computed using Equation (2).

$$\begin{aligned} \text{RMSE} &= \sqrt{\frac{\sum(\hat{y}-y)^2}{N}} & \text{NSE} &= 1-\frac{\sum(\hat{y}-y)^2}{\sum(y-\bar{y})^2} \\ \text{MAE} &= \frac{100}{N}\sum\left|\frac{y-\bar{y}}{y}\right| & \text{R} &= \frac{\sum(\hat{y}-\bar{\hat{y}})(y-\bar{y})}{\sqrt{\sum(\hat{y}-\bar{\hat{y}})^2}\sqrt{\sum(y-\bar{y})^2}} \end{aligned} \tag{2}$$

Table 6 compares these metrics (including MSE) based on all data points obtained from the networks. As seen, there is a good consistency among those five metrics for five meta-models. For example, higher R corresponds with lower RMSE.

Table 6. Comparison of five statistical indicators to evaluate the accuracy of meta-models.

	MSE	RMSE	NSE	MAE	R
P; SPSW	0.0014	0.0374	0.9796	0.0224	0.9939
K; SPSW	0.0024	0.0489	0.9632	0.022	0.9824
P; RCSW	0.0015	0.0389	0.9375	0.0255	0.9622
K; RCSW	0.0028	0.0534	0.79	0.0278	0.8992
D; RCSW	0.0067	0.082	0.7277	0.0585	0.8479

5.3. Sensitivity Analysis

To evaluate the relative importance of the parameters in the network, the Garson's factor was used [78]. The equation provided for the network with a hidden layer is:

$$Q_{ik} = \frac{\sum_{j=1}^{L}\left(\frac{w_{ij}}{\sum_{r=1}^{N} w_{rj}} v_{jk}\right)}{\sum_{i=1}^{N}\left(\sum_{j=1}^{L}\frac{w_{ij}}{\sum_{r=1}^{N} w_{rj}} v_{jk}\right)} \quad (3)$$

where $\sum_{r=1}^{N} w_{rj}$ is the sum of the connection weights between the N input neurons and the hidden neuron j, and v_{jk} is connection weight between the hidden neuron j and the output neuron k [79].

Sensitivity of each parameter is then presented in Figure 7. The first (and the most important) observation is that nearly all the parameters are contributing effectively in the overall performance of the SWs. Among them, the column's moment of inertia and ultimate stress of the infill plate have most dominant effects. Strength and lateral stiffness of a SPSW depend on the development of diagonal tension field in the infill plate. To develop a uniform diagonal tension field, the boundary elements should have enough flexural stiffness to anchor the tension field [80]. As a result, the flexural stiffness of the boundary elements will have the greatest impact on the load bearing capacity (as seen in this figure). Due to the yielding of the infill plate during loading, its ultimate stress also affects the behavior of the SPSW. Moreover, the thickness and width of the infill plate have significant contribution in the strength. Therefore, the proposed ANN can accurately estimate the behavior of SPSWs. On the other hand, the most important parameters affecting the strength, stiffness and drift ratio of RCSWs are the wall's length (effectiveness = 17.8%), the wall's height (effectiveness = 14.6%), and the horizontal column's reinforcement ratio (effectiveness = 10.3%).

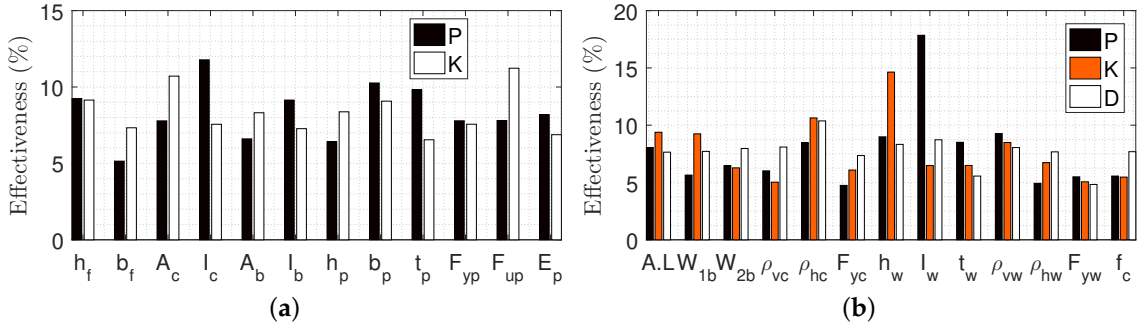

Figure 7. Relative importance of the input parameters in shear wall meta-model. (**a**) SPSW, (**b**) RCSW.

6. Conclusions

Understanding the complex behavior of the shear walls through their effective parameters can help to properly determine the lateral response of the structures. In this paper, an efficient computational method was proposed to estimate the strength, stiffness, and drift ratio of the steel plate and reinforced concrete shear walls from a rich library of experimental data. Over 100 papers and reports were synthesized and the available information were extracted. The parameters were mainly related to the

geometry of the shear walls (such as height, width and thickness of the plate and its surrendering frame), as well as the applied loads, and the material properties. On the other hand, the output was only considered the global behavior of the system (in terms of the stiffness, strength and drift). One may notice that the reinforcement detailing, collapse modes, and buckling parameters were not considered in this meta-modeling. The main reason can be attributed to unavailability of those information in majority of cases. In addition, the failure mode and crack pattern had more qualitative nature, and it was difficult (if not impossible) to present them in a quantitative format (using damage index concept). An artificial neural network was proposed to solve the problem. In this network, the back propagation algorithm was adopted. The network of a single hidden layer with 6 and 10 neurons would have the best performance for SPSW and RCSW, respectively. The major conclusions can be summarized as follows:

- The MSE of test data to estimate the strength and stiffness of the SPSW was 0.000227 and 0.0108, respectively, which indicate the proper performance of the network.
- The MSE of test data in RCSW was 0.0012, 0.0061, and 0.0056 for strength, stiffness and drift ratio, respectively.
- Sensitivity analysis was performed to determine the relative importance of the input parameters on the shear wall's behavior. It was observed that the stiffness of the vertical boundary elements and the ultimate stresses of the infill plate had largest effect on the strength and stiffness of the SPSW, respectively.
- On the other hand, the most important parameters affecting the strength, stiffness and drift ratio of RCSWs were wall's length, wall's height, and the horizontal column's reinforcement ratio, respectively.
- The performance of the network based on different statistical indicators was also found to be very close.

Finally, the detailed values of the ANN weights are provided (see Appendix B). The proposed network can be used to design new walls, retrofit the existing ones, and validate the finite element models. In design level, the proposed network can provide an estimation of the ultimate strength and stiffness values, which can be further correlated with codified values. This is beyond the conventional design philosophy, which is based on linear elastic models. On the other hand, the performance of existing shear walls can be controlled with this meta-model to make sure they have a safe/proper behavior under the target loads, and, if not, they can be retrofitted.

Author Contributions: Conceptualization, M.J.M. and M.A.H.-A.; methodology, M.J.M. and M.A.H.-A.; software, M.J.M.; validation, M.J.M.; formal analysis, M.J.M.; investigation, M.J.M. and M.A.H.-A.; resources, M.J.M. and M.A.H.-A.; data curation, M.J.M.; writing—original draft preparation, M.J.M.; writing—review and editing, M.A.H.-A.; visualization, M.J.M. and M.A.H.-A.; supervision, M.A.H.-A.; project administration, M.A.H.-A.; funding acquisition, M.A.H.-A.

Funding: This research received no external funding.

Acknowledgments: The author would like to thank the editor and reviewers for their helpful and constructive comments that greatly contributed to improving the final version of the paper.

Conflicts of Interest: The authors declare no conflict of interest.

Appendix A. Details of Shear Wall Library

Table A1. Library of steel plate shear walls information.

Reference	hf mm	bf mm	Ac mm^2	Ic mm^4	Ab mm^2	Ib mm^4	hp mm	bp mm	tp mm	Fyp Pa	Fup Pa	Ep Pa	P N	K N/mm
Sigariyazd et al. [81]	1100	1400	7.05×10^3	3.86×10^7	4.10×10^3	1.13×10^7	1020	1200	1.50	2.22×10^8	3.15×10^8	2.00×10^{11}	7.15×10^5	9.63×10^4
Shekastehband et al. [82]	620	620	3.40×10^3	8.64×10^5	3.40×10^3	8.64×10^5	500	460	0.50	1.38×10^8	2.81×10^8	2.00×10^{11}	1.15×10^4	2.38×10^3
Shekastehband et al. [82]	620	620	3.40×10^3	8.64×10^5	3.40×10^3	8.64×10^5	500	460	1.25	1.82×10^8	3.28×10^8	2.00×10^{11}	3.13×10^4	4.69×10^3
Berman et al. [83]	1830	3660	1.82×10^4	3.47×10^8	1.63×10^4	6.37×10^8	1350	3340	1.00	2.15×10^8	4.66×10^8	1.60×10^{11}	3.64×10^5	1.06×10^5
Yu et al. [84]	1250	1350	5.12×10^3	2.88×10^7	2.72×10^3	1.84×10^7	1050	1180	5.00	3.15×10^8	4.78×10^8	2.00×10^{11}	7.08×10^5	2.98×10^4
Choi and Park [85]	1075	1650	9.90×10^3	5.53×10^7	5.80×10^3	3.25×10^7	1000	1500	4.00	2.40×10^8	4.00×10^8	2.00×10^{11}	1.39×10^6	7.00×10^4
Choi and Park [85]	1075	2350	9.90×10^3	5.53×10^7	5.80×10^3	3.25×10^7	1000	2200	4.00	2.40×10^8	4.00×10^8	2.00×10^{11}	1.82×10^6	1.07×10^5
Choi and Park [85]	1075	2350	7.20×10^3	2.40×10^7	5.80×10^3	3.25×10^7	1000	2200	4.00	2.40×10^8	4.00×10^8	2.00×10^{11}	1.57×10^6	1.03×10^5
Wang et al. [86]	1100	2050	9.40×10^3	7.15×10^7	6.35×10^3	4.72×10^7	1000	1800	6.00	4.18×10^8	5.63×10^8	1.98×10^{11}	1.66×10^6	1.07×10^5
Wang et al. [86]	1100	2400	8.10×10^3	9.77×10^7	6.35×10^3	4.72×10^7	1000	2160	6.00	4.18×10^8	5.63×10^8	1.98×10^{11}	1.55×10^6	9.25×10^4
Wang et al. [86]	1100	2400	8.10×10^3	9.77×10^7	6.35×10^3	4.72×10^7	1000	2400	6.00	4.18×10^8	5.63×10^8	1.98×10^{11}	1.64×10^6	7.87×10^4
Sabouri-Ghomi and Sajjadi [87]	1105	1500	5.40×10^3	6.34×10^6	1.06×10^4	1.28×10^8	960	1410	2.00	1.92×10^8	2.77×10^8	2.00×10^{11}	5.74×10^5	1.81×10^5
Chen and Jhang [88]	1500	1500	8.34×10^3	1.33×10^7	8.34×10^3	1.33×10^7	1200	1200	15.00	8.54×10^7	2.58×10^8	1.75×10^{11}	1.35×10^6	N.A.
Chen and Jhang [88]	1500	1500	8.34×10^3	1.33×10^7	8.34×10^3	1.33×10^7	1200	1200	8.00	9.28×10^7	2.72×10^8	1.75×10^{11}	5.59×10^5	N.A.
Nateghi-Alahi and Khazaei-Poul [89]	500	500	2.70×10^3	4.12×10^6	2.70×10^3	4.12×10^6	380	3800	0.90	1.97×10^8	3.23×10^8	2.04×10^{11}	8.26×10^4	2.62×10^4
Caccese et al. [90]	838	1245	2.48×10^3	4.70×10^6	1.08×10^3	1.05×10^6	762	1140	0.76	3.06×10^8	3.47×10^8	1.75×10^{11}	1.69×10^5	1.42×10^4
Caccese et al. [90]	1245	2477	4.70×10^6	1.08×10^3	1.05×10^6	7.62×10^2	1140	1140	1.90	2.91×10^8	3.15×10^8	1.75×10^{11}	3.34×10^5	2.01×10^4
Caccese et al. [90]	1245	2477	4.70×10^6	1.08×10^3	1.05×10^6	7.62×10^2	1140	1140	2.66	2.95×10^8	4.04×10^8	1.75×10^{11}	3.78×10^5	2.66×10^4
Alavi and Nateghi [91]	1366	1960	5.43×10^3	2.49×10^7	5.43×10^3	2.49×10^7	1102	1720	0.80	2.80×10^8	5.00×10^8	2.04×10^{11}	7.65×10^5	1.52×10^4
Park et al. [92]	1100	2250	1.50×10^4	2.09×10^8	9.60×10^3	8.55×10^7	1500	1000	2.00	2.40×10^8	4.00×10^8	1.49×10^{11}	1.72×10^6	8.70×10^4
Park et al. [92]	1100	2250	1.50×10^4	2.09×10^8	9.60×10^3	8.55×10^7	1500	1000	4.00	3.30×10^8	4.90×10^8	1.49×10^{11}	2.53×10^6	1.11×10^5
Park et al. [92]	1100	2250	1.50×10^4	2.09×10^8	9.60×10^3	8.55×10^7	1500	1000	6.00	3.30×10^8	4.90×10^8	1.49×10^{11}	3.02×10^6	1.24×10^5
Park et al. [92]	1100	2250	8.25×10^3	1.15×10^8	9.60×10^3	8.55×10^7	1500	1000	4.00	3.30×10^8	4.90×10^8	1.49×10^{11}	1.53×10^6	9.30×10^4
Park et al. [92]	1100	2250	8.25×10^3	1.15×10^8	9.60×10^3	8.55×10^7	1500	1000	6.00	3.30×10^8	4.90×10^8	1.49×10^{11}	1.68×10^6	1.01×10^5
Lubell et al. [93]	900	900	1.07×10^3	1.04×10^6	1.07×10^3	1.04×10^6	800	800	1.50	3.20×10^8	N.A.	N.A.	2.66×10^5	3.80×10^4
Roberts and Sabouri-Ghomi [94]	370	370	N.A.	N.A.	N.A.	N.A.	300	300	0.83	2.19×10^8	3.28×10^8	2.02×10^{11}	5.17×10^4	N.A.
Roberts and Sabouri-Ghomi [94]	370	370	N.A.	N.A.	N.A.	N.A.	300	300	1.23	1.52×10^8	2.28×10^6	2.03×10^{11}	6.83×10^4	N.A.
Roberts and Sabouri-Ghomi [94]	370	370	N.A.	N.A.	N.A.	N.A.	300	450	0.83	2.19×10^8	3.28×10^8	2.02×10^{11}	6.25×10^4	N.A.
Roberts and Sabouri-Ghomi [94]	370	370	N.A.	N.A.	N.A.	N.A.	300	450	1.23	1.52×10^8	2.28×10^6	2.03×10^{11}	7.52×10^4	N.A.

Table A2. Library of reinforced concrete shear walls information.

Reference	A.L kN	ac mm	bc mm	ρ_{vc} %	ρ_{hc} %	Fyc MPa	hw mm	lw mm	tw mm	ρ_{vw} %	ρ_{hw} %	Fyw MPa	Fcw MPa	P kN	K kN/mm	D %
Carrillo et al. [95]	60	102	102	0.670	0.420	434.0	2426	2402	102	0.140	0.140	447.0	18.80	408.0	N.A.	2.01
Carrillo et al. [95]	60	101	101	0.980	0.420	430.0	2426	2402	101	0.280	0.280	447.0	18.80	617.0	N.A.	1.71
Carrillo et al. [95]	60	102	102	0.680	0.420	434.0	2423	2399	102	0.140	0.140	447.0	17.50	352.0	N.A.	1.03
Carrillo et al. [95]	60	101	101	0.980	0.420	430.0	2421	2397	101	0.280	0.280	447.0	17.50	453.0	N.A.	1.72
Carrillo et al. [95]	60	100	100	0.220	0.430	443.0	2430	5400	100	0.280	0.280	447.0	16.20	766.0	N.A.	1.05
Carrillo et al. [95]	60	103	103	0.220	0.410	456.0	2430	5396	103	0.120	0.120	605.0	20.00	776.0	N.A.	0.45
Carrillo et al. [95]	60	103	103	0.720	0.420	443.0	2422	2398	103	0.120	0.120	605.0	20.00	329.0	N.A.	0.54
Carrillo et al. [95]	60	101	101	0.960	0.420	443.0	2478	1239	101	0.120	0.120	605.0	20.00	154.0	N.A.	0.68
Carrillo et al. [95]	60	83	83	0.780	0.430	411.0	1916	1916	83	0.110	0.110	630.0	24.70	234.0	68.6	0.54
Carrillo et al. [95]	60	84	84	1.020	0.420	411.0	1921	1921	84	0.260	0.260	435.0	24.70	274.0	72	1.51
Yuan et al. [96]	1527	200	200	0.370	0.800	473.0	2360	1280	200	0.390	0.330	544.0	45.90	656.0	N.A.	1.14
Yuan et al. [96]	1527	200	200	0.370	0.800	473.0	2360	1280	200	0.710	0.710	544.0	45.90	740.0	N.A.	1.15
Shiga et al. [97]	0	150	120	0.049	0.089	390.0	600	1000	50	0.250	0.250	300.0	16.00	177.0	N.A.	2.40
Shiga et al. [97]	0	150	120	0.049	0.089	390.0	600	1000	50	0.250	0.250	300.0	16.00	188.0	N.A.	2.40
Shiga et al. [97]	0	150	120	0.049	0.089	390.0	600	1000	50	0.250	0.250	300.0	16.00	211.0	N.A.	2.40
Shiga et al. [97]	0	150	120	0.049	0.089	390.0	600	1000	50	0.250	0.250	300.0	16.00	231.0	N.A.	4.28
Shiga et al. [97]	200	150	120	0.049	0.089	390.0	600	1000	50	0.250	0.250	300.0	16.00	341.0	N.A.	4.28
Shiga et al. [97]	0	150	120	0.049	0.089	390.0	600	1000	50	0.500	0.500	300.0	16.00	240.0	N.A.	2.34
Shiga et al. [97]	200	150	120	0.049	0.089	390.0	600	1000	50	0.500	0.500	300.0	16.00	310.0	N.A.	2.32
Shiga et al. [97]	400	150	120	0.049	0.089	390.0	600	1000	50	0.500	0.500	300.0	16.00	287.0	N.A.	2.40
Greifenhagen and Lestuzzi [98]	136	100	100	0.300	0.300	504.0	610	1000	100	0.300	0.300	504.0	50.70	204.0	333	3.50
Greifenhagen and Lestuzzi [98]	136	100	100	0.300	0.000	504.0	610	1000	100	0.300	0.000	504.0	51.00	203.0	111	2.50
Greifenhagen and Lestuzzi [98]	136	80	80	0.300	0.300	745.0	610	900	80	0.300	0.300	745.0	20.10	176.0	108	1.70
Greifenhagen and Lestuzzi [98]	136	80	80	0.300	0.300	745.0	610	900	80	0.300	0.300	745.0	24.40	135.0	125	2.00
Looi et al. [99]	220	80	80	2.000	1.400	601.0	800	800	80	2.000	1.400	601.0	29.10	252.5	170	1.11
Looi et al. [99]	380	80	80	2.000	1.400	601.0	800	800	80	2.000	1.400	601.0	26.40	245.0	160	1.03
Looi et al. [99]	680	80	80	2.000	1.400	601.0	800	800	80	2.000	1.400	601.0	27.60	249.3	171	0.63
Looi et al. [99]	780	80	80	2.000	1.400	601.0	800	800	80	2.000	1.400	601.0	28.00	250.9	200	0.47
Lopes [100]	96	45	115	4.120	0.800	436.0	495	450	45	0.620	0.400	414.0	45.00	108.3	14.4	2.12
Lopes [100]	70	45	115	4.120	5.000	436.0	495	450	45	0.620	2.800	414.0	44.50	80.3	19.6	1.65
Lopes [100]	80	45	115	4.120	4.000	436.0	495	450	45	0.620	2.000	414.0	45.10	83.6	17.5	2.52
Yanez et al. [101]	0	120	120	0.500	0.400	475.0	2300	2000	120	0.500	0.400	475.0	34.00	287.0	37.5	6.20
Bouchon et al. [102]	150	180	100	2.500	0.070	565.0	750	1500	100	0.300	0.300	585.0	31.70	550.0	N.A.	N.A.
Bouchon et al. [102]	150	180	100	2.500	0.070	565.0	750	1500	100	0.500	0.500	615.0	36.40	645.0	N.A.	N.A.

Table A2. *Cont.*

Reference	A.L kN	ac mm	bc mm	ρ_{vc} %	ρ_{hc} %	Fyc MPa	hw mm	lw mm	tw mm	ρ_{vw} %	ρ_{hw} %	Fyw MPa	Fcw MPa	P kN	K kN/mm	D %
Bouchon et al. [102]	150	180	100	2.500	0.070	565.0	750	1500	100	0.800	0.800	620.0	28.60	853.0	N.A.	N.A.
Tasnimi [103]	0	50	80	2.800	0.250	276.0	1500	500	50	0.250	0.250	216.0	21.6 cy	15.4	3.29	1.10
Tasnimi [103]	0	50	80	2.800	0.250	276.0	1500	500	50	0.250	0.250	216.0	21.60	19.6	4.5	0.75
Tasnimi [103]	0	50	80	2.800	0.250	276.0	1500	500	50	0.250	0.250	216.0	22.45	17.5	4.1	1.03
Tasnimi [103]	0	50	80	2.800	0.250	276.0	1500	500	50	0.250	0.250	216.0	23.45	19.8	3.5	0.90
Lefas et al. [104]	0	70	140	3.100	1.200	470.0	750	750	70	2.400	1.100	470.0	52.3 Cu	260.0	102.9	1.10
Lefas et al. [104]	230	70	140	3.100	1.200	470.0	750	750	70	2.400	1.100	470.0	53.60	340.0	173	1.18
Lefas et al. [104]	355	70	140	3.100	1.200	470.0	750	750	70	2.400	1.100	470.0	40.60	330.0	135.1	1.18
Lefas et al. [104]	0	70	140	3.100	1.200	470.0	750	750	70	2.400	1.100	470.0	42.10	265.0	102.9	1.49
Lefas et al. [104]	185	70	140	3.100	1.200	470.0	750	750	70	2.400	1.100	470.0	43.30	320.0	166.6	1.07
Lefas et al. [104]	460	70	140	3.100	1.200	470.0	750	750	70	2.400	1.100	470.0	51.70	355.0	200	0.77
Lefas et al. [104]	0	70	140	3.100	1.200	470.0	750	750	70	2.400	0.370	470.0	48.30	247.0	65.7	1.43
Lefas et al. [104]	0	65	140	3.300	0.900	470.0	1300	650	65	2.500	0.800	470.0	42.80	127.0	31.25	1.58
Lefas et al. [104]	182	65	140	3.300	0.900	470.0	1300	650	65	2.500	0.800	470.0	50.60	150.0	35.9	1.17
Lefas et al. [104]	343	65	140	3.300	0.900	470.0	1300	650	65	2.500	0.800	470.0	47.80	180.0	38.4	1.01
Lefas et al. [104]	0	65	140	3.300	0.900	470.0	1300	650	65	2.500	0.800	470.0	48.30	120.0	34.4	1.39
Lefas et al. [104]	325	65	140	3.300	0.900	470.0	1300	650	65	2.500	0.800	470.0	45.00	150.0	62.5	0.73
Lefas et al. [104]	0	65	140	3.300	0.900	470.0	1300	650	65	2.500	0.400	470.0	30.10	123.0	25.6	1.61
Lefas and Kotsovos [105]	0	65	140	3.300	0.900	470.0	1300	650	65	1.500	0.350	470.0	30.10	117.7	11.4	1.61
Lefas and Kotsovos [105]	0	65	140	3.300	0.900	470.0	1300	650	65	1.500	0.350	470.0	35.20	115.8	11.42	1.70
Lefas and Kotsovos [105]	0	65	140	3.300	0.900	470.0	1300	650	65	1.500	0.350	470.0	53.60	111.0	8	1.88
Lefas and Kotsovos [105]	0	65	140	3.300	0.900	470.0	1300	650	65	1.500	0.350	470.0	49.20	111.5	10	1.92
Pilakoutas and Elnashai [106]	0	110	60	2.830	0.780	500.0	1200	600	60	0.310	0.390	550.0	36.90	104.0	19.3	2.00
Pilakoutas and Elnashai [106]	0	60	60	3.020	0.170	540.0	1200	600	60	0.470	0.310	550.0	31.80	117.3	21.7	0.80
Pilakoutas and Elnashai [106]	0	110	60	2.830	0.170	500.0	1200	600	60	0.310	0.310	550.0	38.60	107.8	20	1.83
Pilakoutas and Elnashai [106]	0	60	60	3.020	0.780	540.0	1200	600	60	0.470	0.390	550.0	32.00	127.3	21.3	1.83
Pilakoutas and Elnashai [106]	0	110	60	2.930	0.410	540.0	1200	600	60	0.310	0.310	550.0	45.80	95.3	18.6	2.16
Pilakoutas and Elnashai [106]	0	110	60	2.930	0.450	540.0	1200	600	60	0.310	0.310	550.0	38.90	97.4	18.7	2.16
Gupta and Rangan [107]	0	375	100	1.250	0.150	545.0	1000	1000	75	1.000	0.500	545.0	79.30	427.8	N.A.	N.A.
Gupta and Rangan [107]	610	375	100	1.730	0.150	545.0	1000	1000	75	1.000	0.500	545.0	65.10	719.6	N.A.	N.A.
Gupta and Rangan [107]	1230	375	100	2.140	0.150	545.0	1000	1000	75	1.000	0.500	545.0	69.00	850.7	N.A.	N.A.
Gupta and Rangan [107]	0	375	100	1.840	0.150	533.2	1000	1000	75	1.500	0.500	533.2	75.20	600.0	N.A.	N.A.
Gupta and Rangan [107]	610	375	100	2.260	0.150	533.2	1000	1000	75	1.500	0.500	533.2	73.10	790.2	N.A.	N.A.
Gupta and Rangan [107]	1230	375	100	2.490	0.150	533.2	1000	1000	75	1.500	0.500	533.2	70.50	970.0	N.A.	N.A.

Table A2. *Cont.*

Reference	A.L kN	ac mm	bc mm	ρ_{vc} %	ρ_{hc} %	Fyc MPa	hw mm	lw mm	tw mm	ρ_{vw} %	ρ_{hw} %	Fyw MPa	Fcw MPa	P kN	K kN/mm	D %
Gupta and Rangan [107]	610	375	100	1.730	0.150	545.0	1000	1000	75	1.000	1.000	545.0	71.20	800.0	N.A.	N.A.
Gupta and Rangan [107]	310	375	100	0.630	0.150	545.0	1000	1000	75	1.000	0.500	545.0	60.50	486.6	N.A.	N.A.
Mickleborough et al. [108]	357	0	0	0.000	0.000	0.0	1500	750	125	1.170	0.390	460.0	44.70	156.0	70.52	0.43
Mickleborough et al. [108]	493	0	0	0.000	0.000	0.0	1500	750	125	1.170	0.390	460.0	56.00	235.0	56.55	0.66
Mickleborough et al. [108]	334	0	0	0.000	0.000	0.0	1125	750	125	1.170	0.390	460.0	29.50	217.0	105.81	0.45
Mickleborough et al. [108]	486	0	0	0.000	0.000	0.0	1125	750	125	1.170	0.390	460.0	57.30	289.0	173.61	0.43
Mickleborough et al. [108]	360	0	0	0.000	0.000	0.0	750	750	125	1.170	0.390	460.0	57.30	420.0	269.2	0.54
Mickleborough et al. [108]	477	0	0	0.000	0.000	0.0	750	750	125	1.170	0.390	460.0	29.50	400.0	284	0.93
Sittipunt et al. [109]	0	250	250	2.290	0.540	473.0	1900	1000	100	0.390	0.520	450.0	36.60	491.0	137.8	2.90
Sittipunt et al. [109]	0	250	250	2.290	0.540	473.0	1900	1000	100	0.520	0.790	450.0	35.80	608.0	185	2.80
Zhang and Wang [110]	500	100	100	0.009	0.010	405.0	1500	700	100	0.007	0.010	405.0	36.80	201.2	49.79	2.08
Zhang and Wang [110]	784	100	100	0.007	0.010	432.0	1500	700	100	0.007	0.010	432.0	40.20	224.0	54	1.59
Zhang and Wang [110]	595	100	100	0.018	0.010	375.0	1500	700	100	0.007	0.010	375.0	43.10	303.5	52.14	2.10
Adebar et al. [111]	1500	380	203	0.670	1.700	455.0	11760	1625	127	0.270	0.270	455.0	49.00	160.0	42	2.39
Terzioglu et al. [112]	0	120	250	5.150	0.680	440.0	750	1500	120	0.680	0.680	481.0	19.30	799.0	338	1.20
Terzioglu et al. [112]	0	120	250	5.150	0.680	440.0	750	1500	120	0.680	0.680	481.0	25.80	666.0	282	1.20
Terzioglu et al. [112]	0	120	250	5.150	0.680	473.0	750	1500	120	0.680	0.680	584.0	29.00	813.0	506.6	1.20
Terzioglu et al. [112]	0	120	250	5.150	0.680	584.0	750	1500	120	0.680	0.680	584.0	32.10	383.0	340	1.20
Terzioglu et al. [112]	0	120	250	5.150	0.680	519.0	500	1500	120	0.680	0.680	584.0	34.80	874.0	1440	1.40
Terzioglu et al. [112]	0	120	250	5.150	0.340	528.0	1500	1500	120	0.680	0.340	584.0	35.00	710.0	226	1.60
Terzioglu et al. [112]	0	120	250	5.150	0.680	528.0	1500	1500	120	0.680	0.680	584.0	22.60	735.0	186	1.40
Terzioglu et al. [112]	0	120	90	5.150	0.340	473.0	750	1500	120	0.340	0.340	584.0	24.00	563.0	426.6	1.20
Terzioglu et al. [112]	240	120	90	5.150	0.340	473.0	750	1500	120	0.340	0.340	584.0	26.30	789.0	800	1.20
Terzioglu et al. [112]	480	120	90	5.150	0.340	473.0	750	1500	120	0.340	0.340	584.0	27.00	793.0	733.33	1.20
Terzioglu et al. [112]	0	120	90	5.150	0.340	440.0	750	1500	120	0.340	0.340	481.0	23.70	635.0	480	1.20
Abdulridha and Palermo [113]	0	160	150	1.300	1.700	410.0	2200	1000	150	0.880	0.880	425.0	30.50	156.0	12.34	3.20
Qazi et al. [114]	110	0	0	0.300	0.200	500.0	610	900	80	0.300	0.200	500.0	35.00	138.0	37.93	1.21
Christidis and Trezos [115]	0	0	0	14.330	6.690	588.0	1400	750	125	14.330	6.690	588.0	31.12	203.0	16.8	3.70
Christidis and Trezos [115]	0	0	0	12.060	2.010	580.0	1400	750	125	12.060	2.010	580.0	31.12	177.0	11.69	3.60
Christidis and Trezos [115]	0	0	0	12.060	1.130	580.0	1400	750	125	12.060	1.130	580.0	31.12	173.3	15.7	3.60
Christidis and Trezos [115]	0	0	0	12.060	1.130	580.0	1400	750	125	12.060	1.130	580.0	25.37	157.6	14.08	2.14
Wang et al. [116]	1800	0	0	0.310	0.310	347.8	2000	1000	125	0.310	0.310	347.8	28.76	233.0	31.38	0.50
Wang et al. [116]	1438	0	0	0.310	0.310	347.8	2000	1000	125	0.310	0.310	347.8	28.76	212.0	32.54	0.70
Wang et al. [116]	2978	0	0	0.190	0.190	347.8	2000	1000	200	0.190	0.190	347.8	49.64	371.0	49.16	1.25

Table A2. *Cont.*

Reference	A.L kN	ac mm	bc mm	ρ_{vc} %	ρ_{hc} %	Fyc MPa	hw mm	lw mm	tw mm	ρ_{vw} %	ρ_{hw} %	Fyw MPa	Fcw MPa	P kN	K kN/mm	D %
Ren et al. [117]	1400	180	180	3.140	0.310	432.0	1700	925	180	0.220	0.620	312.0	44.30	549.0	83.7	2.59
Hariri-Ardebili and Saouma [19]	800	200	120	2.100	0.670	430.0	750	1300	100	0.800	0.770	430.0	79.00	1180.0	500	0.94
Le Nguyen et al. [118]	110	0	0	0.160	0.130	500.0	610	900	80	0.160	0.130	500.0	35.93	158.0	153	0.98
Le Nguyen et al. [118]	90	0	0	0.180	0.100	500.0	1500	600	80	0.180	0.100	500.0	34.65	25.0	20.6	0.86
Choi [119]	300	200	200	1.420	1.300	400.0	950	1500	100	0.460	0.530	400.0	37.26	610.0	104.8	1.70
Choi [119]	300	200	200	1.420	1.300	400.0	950	1500	100	0.870	0.480	400.0	41.91	695.0	109.6	1.89
Choi [119]	300	200	200	1.420	1.300	400.0	950	1500	100	0.460	1.850	400.0	40.34	620.0	117.1	1.57
Choi [119]	300	200	200	1.420	1.300	400.0	950	1500	100	0.460	1.850	400.0	40.34	650.0	91.62	1.78
Cortés-Puentes and Palermo [120]	0	0	0	0.180	0.210	495.0	2000	2000	100	0.180	0.210	495.0	22.50	145.0	24.2	1.85
Cortés-Puentes and Palermo [121]	0	0	0	0.180	0.210	495.0	2000	2000	100	0.180	0.210	495.0	9.50	117.0	25.7	2.00
Cortés-Puentes and Palermo [122]	0	225	225	1.000	0.510	495.0	2000	1550	125	0.180	0.200	495.0	20.00	243.0	105.3	1.50
Qiao et al. [123]	100	160	160	0.785	0.220	338.2	850	1000	160	0.250	0.120	535.8	26.48	338.3	794	2.93
Blandon et al. [124]	470	350	100	1.000	0.140	419.0	2400	2500	100	0.270	0.270	419.0	39.10	323.7	203.4	0.80
Blandon et al. [124]	470	350	100	1.000	0.140	419.0	2400	2500	100	0.260	0.260	419.0	40.10	320.0	61.73	1.20
Blandon et al. [124]	470	350	100	1.780	0.140	419.0	2400	2500	100	0.270	0.270	419.0	39.20	324.3	130	0.92
Christidis et al. [125]	0	0	0	1.200	0.110	580.0	1400	750	125	1.200	0.110	580.0	25.37	157.6	14.08	2.20
Liao et al. [126]	300	170	170	2.780	0.590	387.0	820	860	85	0.550	0.550	397.0	49.20	636.0	1630	2.00
Liao et al. [126]	300	170	170	2.780	0.590	387.0	820	1320	85	0.550	0.550	397.0	49.20	852.0	794	1.28
Liao et al. [126]	600	170	170	2.780	0.590	387.0	820	1320	85	0.550	0.550	397.0	49.20	966.0	564.6	1.12
Dazio et al. [127]	689	150	150	1.570	1.430	547.0	4030	2000	150	0.300	0.250	583.0	45.00	336.0	47.3	1.04
Dazio et al. [127]	691	150	150	1.570	1.590	583.0	4030	2000	150	0.300	0.250	484.0	40.50	359.0	64.9	1.38
Dazio et al. [127]	686	150	230	1.300	1.210	601.0	4030	2000	150	0.540	0.250	569.0	39.20	454.0	113	2.03
Dazio et al. [127]	695	0	0	0.000	0.000	576.0	4030	2000	150	0.540	0.250	583.0	40.90	443.0	69	1.35
Dazio et al. [127]	1474	150	230	0.670	0.390	576.0	4030	2000	150	0.270	0.250	583.0	38.30	439.0	64.4	1.36
Dazio et al. [127]	1476	150	355	1.540	0.820	576.0	3990	2000	150	0.540	0.250	583.0	45.60	597.0	87.9	2.07
Zhi et al. [128]	600	200	385	1.200	0.780	510.0	3450	1600	200	0.860	0.390	505.0	41.20	482.0	22.4	2.23
Zhi et al. [128]	600	200	407	1.130	1.200	510.0	3450	1600	200	0.860	0.390	505.0	42.10	448.0	22.9	2.05
Zhi et al. [128]	600	200	407	1.130	1.200	510.0	3450	1600	200	0.860	0.390	505.0	42.10	462.0	26.8	2.05
Zhi et al. [128]	600	200	407	1.130	1.600	510.0	3450	1600	200	0.860	0.390	505.0	42.10	439.0	26.8	1.80
Zhi et al. [128]	600	200	407	1.130	1.600	510.0	3450	1600	200	0.860	0.390	505.0	42.10	456.0	21.9	2.26
Zhi et al. [128]	600	200	407	1.130	1.600	510.0	3450	1600	200	0.860	0.390	505.0	42.10	462.0	21.3	1.80
Zhi et al. [128]	750	200	415	1.940	1.200	510.0	3650	1700	200	1.150	0.390	505.0	41.20	580.0	22.4	2.55
Zhi et al. [128]	750	200	415	1.940	1.200	510.0	3650	1700	200	1.150	0.390	505.0	42.10	605.0	23.4	2.62
Zhi et al. [128]	750	200	415	1.940	1.200	510.0	3650	1700	200	1.150	0.390	505.0	42.10	598.0	17.2	3.03

Table A2. *Cont.*

Reference	A.L kN	ac mm	bc mm	ρ_{vc} %	ρ_{hc} %	Fyc MPa	hw mm	lw mm	tw mm	ρ_{vw} %	ρ_{hw} %	Fyw MPa	Fcw MPa	P kN	K kN/mm	D %
Shen et al. [129]	325	120	225	1.740	0.550	335.0	1600	1000	120	0.600	0.550	235.0	31.00	272.7	14.75	2.50
Zhang et al. [130]	74.85	140	140	0.760	0.250	410.0	1050	1200	140	0.250	0.250	384.0	55.56	400.0	N.A.	2.20
Zhang et al. [130]	134.73	140	140	0.760	0.120	425.0	850	1000	140	0.250	0.250	290.0	22.76	N.A.	N.A.	N.A.
Zhang et al. [130]	67.36	140	140	0.760	0.120	302.0	850	1000	140	0.250	0.250	290.0	45.30	N.A.	N.A.	N.A.
Zhang et al. [130]	112.27	140	140	1.000	0.180	302.0	850	1000	140	0.250	0.125	397.0	24.65	N.A.	N.A.	N.A.
Zhang et al. [130]	112.27	140	140	1.000	0.180	302.0	850	1000	140	0.250	0.250	397.0	24.65	N.A.	N.A.	N.A.
Zhang et al. [130]	112.27	140	140	1.000	0.180	302.0	850	1000	140	0.150	0.150	397.0	24.65	N.A.	N.A.	N.A.
Zhang et al. [130]	112.27	140	140	1.000	0.000	302.0	850	1000	140	0.150	0.150	397.0	24.65	N.A.	N.A.	N.A.
Zhang et al. [130]	112.27	140	140	1.150	0.000	302.0	850	1000	140	0.150	0.150	397.0	24.65	N.A.	N.A.	N.A.
Zhang et al. [130]	112.27	140	140	1.410	0.180	302.0	850	1000	140	0.150	0.150	397.0	24.65	N.A.	N.A.	N.A.
Hidalgo et al. [2]	0	N.A.	N.A.	N.A.	N.A.	N.A.	2000	1000	120	0.251	0.131	392.0	19.40	198.0	130	0.66
Hidalgo et al. [2]	0	N.A.	N.A.	N.A.	N.A.	N.A.	2000	1000	120	0.251	0.246	402.0	19.60	270.0	116.2	0.75
Hidalgo et al. [2]	0	N.A.	N.A.	N.A.	N.A.	N.A.	2000	1000	120	0.251	0.381	402.0	19.50	324.0	79.9	0.75
Hidalgo et al. [2]	0	N.A.	N.A.	N.A.	N.A.	N.A.	1800	1300	120	0.259	0.131	314.0	17.60	309.0	240	0.44
Hidalgo et al. [2]	0	N.A.	N.A.	N.A.	N.A.	N.A.	1800	1300	120	0.125	0.246	471.0	18.10	364.0	137	0.63
Hidalgo et al. [2]	0	N.A.	N.A.	N.A.	N.A.	N.A.	1800	1300	120	0.259	0.246	471.0	15.70	374.0	212.7	0.55
Hidalgo et al. [2]	0	N.A.	N.A.	N.A.	N.A.	N.A.	1800	1300	100	0.255	0.255	366.0	17.60	258.0	59	0.54
Hidalgo et al. [2]	0	N.A.	N.A.	N.A.	N.A.	N.A.	1800	1300	80	0.250	0.250	367.0	16.40	187.0	64.44	0.46
Hidalgo et al. [2]	0	N.A.	N.A.	N.A.	N.A.	N.A.	1400	1400	100	0.255	0.127	362.0	16.30	235.0	218.57	0.35
Hidalgo et al. [2]	0	N.A.	N.A.	N.A.	N.A.	N.A.	1400	1400	100	0.127	0.255	366.0	17.00	304.0	123.21	0.50
Hidalgo et al. [2]	0	N.A.	N.A.	N.A.	N.A.	N.A.	1400	1400	100	0.255	0.255	370.0	18.10	289.0	205.71	0.35
Hidalgo et al. [2]	0	N.A.	N.A.	N.A.	N.A.	N.A.	1200	1700	80	0.250	0.125	366.0	17.10	255.0	239.58	0.25
Hidalgo et al. [2]	0	N.A.	N.A.	N.A.	N.A.	N.A.	1200	1700	80	0.125	0.250	366.0	19.00	368.0	245	0.42
Hidalgo et al. [2]	0	N.A.	N.A.	N.A.	N.A.	N.A.	1200	1700	80	0.250	0.250	366.0	18.80	362.0	169.44	0.37
Hidalgo et al. [2]	0	N.A.	N.A.	N.A.	N.A.	N.A.	1800	1300	100	0.000	0.000	0.0	24.20	258.0	81.81	0.28
Hidalgo et al. [2]	0	N.A.	N.A.	N.A.	N.A.	N.A.	1800	1300	100	0.000	0.000	0.0	17.20	222.0	74.74	0.27
Hidalgo et al. [2]	0	N.A.	N.A.	N.A.	N.A.	N.A.	1800	1300	100	0.000	0.250	431.0	24.20	333.0	75.81	0.36
Hidalgo et al. [2]	0	N.A.	N.A.	N.A.	N.A.	N.A.	1800	1300	100	0.250	0.000	431.0	23.90	323.0	80.09	0.21
Hidalgo et al. [2]	0	N.A.	N.A.	N.A.	N.A.	N.A.	1400	1400	100	0.000	0.000	0.0	23.90	352.0	105.35	0.60
Hidalgo et al. [2]	0	N.A.	N.A.	N.A.	N.A.	N.A.	1400	1400	100	0.000	0.000	0.0	17.70	262.0	90	0.46
Hidalgo et al. [2]	0	N.A.	N.A.	N.A.	N.A.	N.A.	1400	1400	100	0.000	0.250	431.0	23.90	491.0	87.14	0.64
Hidalgo et al. [2]	0	N.A.	N.A.	N.A.	N.A.	N.A.	1400	1400	100	0.250	0.000	431.0	23.30	258.0	119.84	0.31
Hidalgo et al. [2]	0	N.A.	N.A.	N.A.	N.A.	N.A.	1050	1500	80	0.000	0.000	0.0	23.20	400.0	216.19	0.51
Hidalgo et al. [2]	0	N.A.	N.A.	N.A.	N.A.	N.A.	1050	1500	80	0.000	0.000	0.0	17.90	356.0	252.38	0.63

Table A2. *Cont.*

Reference	A.L kN	ac mm	bc mm	ρ_{vc} %	ρ_{hc} %	Fyc MPa	hw mm	lw mm	tw mm	ρ_{vw} %	ρ_{hw} %	Fyw MPa	Fcw MPa	P kN	K kN/mm	D %
Hidalgo et al. [2]	0	N.A.	N.A.	N.A.	N.A.	N.A.	1050	1500	80	0.000	0.250	431.0	23.10	391.0	211.1	0.35
Hidalgo et al. [2]	0	N.A.	N.A.	N.A.	N.A.	N.A.	1050	1500	80	0.250	0.000	431.0	23.30	344.0	206.35	0.38
Ji et al. [131]	617	180	280	5.600	1.500	349.0	1350	1500	180	0.580	0.370	396.3	62.90	960.2	86.3	1.90
Ji et al. [131]	1030	180	280	5.600	1.500	349.0	1350	1500	180	0.580	0.370	396.3	63.40	822.8	76.13	1.70
Ji et al. [131]	1716	180	280	5.600	1.500	349.0	1350	1500	180	0.580	0.370	396.3	63.60	567.5	81.83	1.80
Ji et al. [131]	2553	180	280	5.600	1.500	478.3	1350	1500	180	0.580	0.370	465.0	56.70	460.0	93.14	3.40
Ji et al. [131]	3192	180	280	5.600	1.500	478.3	1350	1500	180	0.580	0.370	465.0	58.10	302.0	23.2	2.30
Ji et al. [131]	0	180	280	5.600	1.500	478.3	1350	1500	180	0.580	0.370	465.0	55.40	1276.0	109.8	1.50
Mohamed et al. [132]	823.2	200	140	0.500	0.630	400.0	3550	1500	200	0.230	0.630	400.0	39.20	476.0	36.5	2.60
Mohamed et al. [132]	838	200	140	1.430	0.890	1412.0	3550	1500	200	0.580	1.580	1412.0	39.90	586.0	26.3	3.10
Mohamed et al. [132]	668.6	200	140	0.000	0.000	1412.0	3550	1200	200	0.620	0.000	1412.0	39.80	449.0	19	3.00
Mohamed et al. [132]	562.8	200	140	0.000	0.000	1412.0	3550	1000	200	0.590	0.000	1412.0	40.20	289.0	13.7	3.35
Quiroz et al. [133]	186	250	100	1.500	0.180	450.0	2400	2650	100	0.180	0.180	450.0	17.16	355.0	170.68	1.08
Quiroz et al. [133]	186	250	100	1.500	0.180	450.0	2400	2650	100	0.180	0.180	450.0	17.16	379.0	170.79	0.48
Quiroz et al. [133]	186	250	100	1.500	0.180	450.0	2400	2650	100	0.180	0.180	450.0	17.16	419.0	201.46	0.78
Quiroz et al. [133]	186	250	100	1.500	0.257	450.0	2400	2650	100	0.257	0.257	450.0	17.16	436.0	216.07	0.71
Quiroz et al. [133]	186	250	100	1.500	0.257	450.0	2400	2650	100	0.257	0.257	450.0	17.16	416.0	227.44	0.53
Quiroz et al. [133]	186	250	100	1.500	0.257	450.0	2400	2650	100	0.257	0.257	450.0	17.16	436.0	215.26	1.41
Quiroz et al. [133]	186	250	100	1.500	0.284	450.0	2400	2650	100	0.284	0.284	450.0	17.16	456.0	217.62	1.04
Salonikios et al. [134]	0	100	240	1.700	1.700	500.0	1200	1200	100	0.565	0.565	500.0	22.20	262.0	131	0.83
Salonikios et al. [134]	0	100	240	1.300	1.700	500.0	1200	1200	100	0.277	0.277	500.0	21.60	191.0	73.46	0.70
Salonikios et al. [134]	200	100	240	1.300	1.700	500.0	1200	1200	100	0.277	0.277	500.0	23.90	268.0	92.4	1.80
Salonikios et al. [134]	0	100	240	1.700	1.100	500.0	1800	1200	100	0.565	0.565	500.0	26.10	197.0	24.32	1.50
Salonikios et al. [134]	0	100	240	1.300	1.100	500.0	1800	1200	100	0.277	0.277	500.0	26.20	124.0	15	1.40
Salonikios et al. [134]	202	100	240	1.300	1.100	500.0	1800	1200	100	0.277	0.277	500.0	24.10	176.0	34	2.05
Salonikios et al. [134]	0	100	240	1.300	1.700	500.0	1800	1200	100	0.565	0.565	500.0	27.50	202.0	16.6	1.50
Thomsen [135]	341	171	102	3.250	1.160	414.0	3660	1220	102	0.280	0.110	414.0	27.40	148.0	10.37	2.20
Thomsen [135]	238	171	102	3.250	1.132	414.0	3660	1220	102	0.280	0.170	414.0	27.40	158.0	10.45	2.40
Tran and Wallace [136]	878	180	150	3.230	0.250	400.0	2440	1220	150	0.270	0.270	400.0	48.00	481.0	74	3.11
Tran and Wallace [136]	878	180	150	7.110	0.250	448.0	2440	1220	150	0.610	0.610	448.0	48.00	742.0	80.47	3.00
Tran and Wallace [136]	878	180	150	3.230	0.250	400.0	1830	1220	150	0.320	0.320	400.0	48.00	603.0	146	3.20
Tran and Wallace [136]	1024	180	150	6.060	0.250	448.0	1830	1220	150	0.730	0.730	448.0	56.00	859.0	134	3.00
Tran and Wallace [136]	256	180	150	6.060	0.250	400.0	1830	1220	150	0.610	0.610	400.0	56.00	670.0	109.2	3.00

Table A2. *Cont.*

Reference	A.L kN	ac mm	bc mm	ρ_{vc} %	ρ_{hc} %	Fyc MPa	hw mm	lw mm	tw mm	ρ_{vw} %	ρ_{hw} %	Fyw MPa	Fcw MPa	P kN	K kN/mm	D %
Layssi and Mitchell [137]	0	0	0	0.830	0.260	460.0	3250	1200	150	0.830	0.260	470.0	31.20	95.2	39.33	0.47
Layssi and Mitchell [137]	0	0	0	1.500	0.260	460.0	3250	1200	150	1.500	0.260	470.0	30.40	140.5	25.12	0.50
Ghorbani-Renani et al. [138]	0	200	150	5.330	0.660	429.0	2700	1300	200	0.600	0.660	440.0	28.30	488.2	39	4.60
Ghorbani-Renani et al. [138]	0	200	150	5.330	0.660	429.0	2700	1300	200	0.600	0.660	440.0	28.30	479.0	39	4.00
Ghorbani-Renani et al. [138]	0	200	60	2.360	0.660	437.0	1140	548	84	0.480	0.660	437.0	47.00	86.7	19.95	3.23
Ghorbani-Renani et al. [138]	0	200	60	2.360	0.660	437.0	1140	548	84	0.480	0.660	437.0	47.00	88.5	19.95	4.00
Ghazizadeh et al. [139]	0	150	240	2.200	2.000	414.0	1800	1800	150	0.600	1.000	414.0	61.00	588.0	200	2.20
Ghazizadeh and Cruz-Noguez [140]	0	150	240	1.050	0.840	1254.0	1800	1800	150	0.560	1.000	1254.0	40.00	550.0	207	2.20
Athanasopoulou [141]	0	101	76.2	5.000	0.530	512.0	1016	1016	101	0.710	0.710	660.0	46.19	362.0	45.44	2.50
Athanasopoulou [141]	0	101	101	9.400	1.000	453.0	1016	1016	101	0.830	0.830	444.0	46.19	476.0	92.64	2.30
Athanasopoulou [141]	0	101	76.2	9.400	0.980	480.0	1320	1016	101	0.710	0.710	660.0	46.88	392.7	45.44	2.20
Athanasopoulou [141]	0	101	101	13.000	1.400	482.0	1320	1016	101	0.670	0.670	463.0	42.74	529.0	125.8	2.20
Athanasopoulou [141]	0	101	101	11.000	1.200	482.0	1320	1016	101	0.500	0.500	463.0	37.92	476.0	83.9	2.40
Tupper [142]	600	152	140	11.000	0.240	450.0	3900	1000	152	0.280	0.490	450.0	38.70	334.0	8.97	2.90
Arafa et al. [143]	0	200	200	1.430	0.890	1372.0	2000	1500	200	0.590	0.510	1372.0	35.00	678.0	294	2.55
Arafa et al. [143]	0	200	200	1.430	0.890	1372.0	2000	1500	200	0.590	0.790	1372.0	35.00	708.0	290	2.80
Arafa et al. [143]	0	200	200	1.430	0.890	1372.0	2000	1500	200	0.590	1.580	1372.0	40.00	912.0	315	3.00
Arafa et al. [143]	0	200	200	1.430	0.890	1372.0	2000	1500	200	0.590	3.560	1372.0	41.00	935.0	323	3.10
Arafa et al. [143]	0	200	200	1.430	0.890	1372.0	2000	1500	200	0.590	0.000	1372.0	38.00	398.0	306	2.20
Arafa et al. [143]	0	200	200	1.430	0.890	1372.0	2000	1500	200	0.000	0.510	1372.0	35.00	482.0	231.6	2.40
G. Oesterle et al. [144]	0	0	0	1.470	0.000	511.6	4570	1910	102	0.310	0.250	511.6	44.71	118.0	13.7	2.30
G. Oesterle et al. [144]	0	0	0	4.000	2.070	450.2	4570	1910	102	0.310	0.250	450.2	46.37	216.0	15.87	2.90
G. Oesterle et al. [144]	0	305	305	1.110	0.000	449.6	4570	1300	102	0.310	0.290	449.6	52.98	271.0	28.6	3.30
G. Oesterle et al. [144]	0	305	305	3.670	0.000	410.3	4570	1300	102	0.630	0.290	410.3	53.60	680.0	33	2.30
G. Oesterle et al. [144]	0	305	305	1.110	1.280	437.8	4570	1300	102	0.310	0.290	437.8	47.29	276.0	25.9	3.90
G. Oesterle et al. [144]	0	305	305	1.110	1.280	450.2	4570	1300	102	0.310	0.290	450.2	45.02	335.0	N.A.	6.90
G. Oesterle et al. [144]	0	305	305	3.670	1.350	444.0	4570	1300	102	0.630	0.290	444.0	45.30	762.0	34	2.70
Oesterle et al. [145]	272.59	305	305	3.670	0.810	440.6	4570	1300	102	0.630	0.290	440.6	21.82	825.5	N.A.	2.80
Oesterle et al. [145]	349.56	305	305	3.670	1.350	457.8	4570	1300	102	1.380	0.290	457.8	49.33	980.0	172	2.70
Oesterle et al. [145]	349.56	305	305	3.670	1.350	447.5	4570	1300	102	0.630	0.290	447.5	41.97	978.0	N.A.	2.90
Oesterle et al. [145]	349.56	305	305	3.670	1.350	429.6	4570	1300	102	0.630	0.290	429.6	44.09	977.0	N.A.	3.00
Oesterle et al. [145]	349.56	305	305	1.670	1.350	447.5	4570	1300	102	0.630	0.290	447.5	45.61	707.0	N.A.	2.80
Shiu et al. [146]	0	106	318	5.000	0.000	473.0	5500	1905	106	0.240	0.360	473.0	23.30	338.6	7.53	2.86

Table A2. *Cont.*

Reference	A.L kN	ac mm	bc mm	ρ_{vc} %	ρ_{hc} %	Fyc MPa	hw mm	lw mm	tw mm	ρ_{vw} %	ρ_{hw} %	Fyw MPa	Fcw MPa	P kN	K kN/mm	D %
JIANG and LU [147]	200	67	95	0.031	0.010	297.0	933	1667	67	0.010	0.010	325.0	18.30	521.8	375	0.66
JIANG and LU [147]	400	67	95	0.031	0.010	297.0	933	1667	67	0.010	0.010	325.0	18.30	587.2	387	0.79
JIANG and LU [147]	0	67	95	0.031	0.010	297.0	933	827	67	0.010	0.010	325.0	19.10	316.3	371.7	0.80
JIANG and LU [147]	200	67	95	0.031	0.010	297.0	933	827	67	0.010	0.010	325.0	19.10	399.5	379.1	0.95
JIANG and LU [147]	400	67	95	0.031	0.010	297.0	933	827	67	0.010	0.010	325.0	19.10	487.9	483	0.87
JIANG and LU [147]	0	67	95	0.031	0.010	297.0	933	827	67	0.010	0.010	325.0	16.60	307.3	300	0.80
JIANG and LU [147]	200	67	95	0.031	0.010	297.0	933	827	67	0.010	0.010	325.0	16.60	381.1	370.2	0.67
JIANG and LU [147]	400	67	95	0.031	0.010	297.0	933	827	67	0.010	0.010	325.0	16.60	469.1	402.4	0.65
JIANG and LU [147]	0	67	95	0.031	0.010	297.0	933	827	67	0.010	0.010	325.0	16.20	307.7	277.9	0.64
JIANG and LU [147]	200	67	95	0.031	0.010	297.0	933	827	67	0.010	0.010	325.0	16.20	393.6	350.7	0.57
JIANG and LU [147]	400	67	95	0.031	0.010	297.0	933	827	67	0.010	0.010	325.0	16.20	473.0	385.1	0.66
Park et al. [148]	970	200	300	9.700	0.000	617.0	1500	1500	200	0.660	0.510	653.0	46.50	2158.0	171	1.00
Park et al. [148]	970	200	300	9.700	0.000	617.0	1500	1500	200	0.660	0.680	653.0	46.50	2298.0	105	1.00
Park et al. [148]	1470	200	300	9.700	0.000	617.0	1500	1500	200	0.660	0.510	653.0	70.30	2085.0	397	0.75
Park et al. [148]	970	300	200	9.700	3.830	617.0	1500	1500	200	0.540	0.510	653.0	46.50	2544.0	542	1.00
Park et al. [148]	970	200	200	9.700	0.000	617.0	1500	1500	200	0.360	0.250	653.0	46.10	1477.0	133	1.00
Park et al. [148]	1470	200	200	9.700	0.000	617.0	1500	1500	200	0.360	0.250	653.0	70.30	1876.0	222	1.00
Park et al. [148]	970	200	200	9.700	2.300	617.0	1500	1500	200	0.360	0.250	653.0	46.50	1915.0	328	0.90
Park et al. [148]	970	200	120	2.000	2.300	653.0	1500	1500	200	0.360	0.250	653.0	46.50	1149.0	139	2.85
Hube et al. [149]	0	0	0	0.800	1.250	500.0	1600	1600	100	0.200	0.200	500.0	28.90	349.0	135.5	0.39
Hube et al. [149]	0	0	0	0.300	1.250	500.0	1600	1600	100	0.200	0.200	500.0	28.90	233.0	78.7	0.75
Hube et al. [149]	0	0	0	0.800	1.250	500.0	1600	1600	100	0.260	0.260	500.0	28.90	471.0	89.5	0.61
Hube et al. [149]	0	0	0	0.800	1.250	500.0	1600	1600	100	0.140	0.140	500.0	28.90	403.0	98	0.55
Hube et al. [149]	0	0	0	0.800	1.250	500.0	1600	1600	100	0.200	0.200	500.0	28.90	357.0	113.8	0.80
Hube et al. [149]	0	0	0	0.800	1.250	500.0	1600	1600	100	0.140	0.140	500.0	28.90	416.0	58.5	0.93
Hube et al. [149]	0	0	0	0.600	1.250	500.0	1600	1600	80	0.250	0.250	500.0	28.90	324.0	171	0.61
Hube et al. [149]	0	0	0	0.600	1.250	500.0	1600	1600	80	0.170	0.170	500.0	28.90	292.0	43	0.65
Hube et al. [149]	0	0	0	0.600	1.250	500.0	1600	1600	80	0.250	0.250	500.0	28.90	336.0	74	1.25
Alarcon et al. [150]	287	100	140	0.450	0.440	469.0	1600	700	100	0.720	0.440	445.0	27.40	144.3	10.06	2.70
Alarcon et al. [150]	479	100	140	0.450	0.440	469.0	1600	700	100	0.720	0.440	445.0	27.40	166.0	15.3	1.80
Alarcon et al. [150]	671.6	100	140	0.450	0.440	469.0	1600	700	100	0.720	0.440	445.0	27.40	185.6	17.4	1.50

Table A2. *Cont.*

Reference	A.L kN	ac mm	bc mm	ρ_{vc} %	ρ_{hc} %	Fyc MPa	hw mm	lw mm	tw mm	ρ_{vw} %	ρ_{hw} %	Fyw MPa	Fcw MPa	P kN	K kN/mm	D %
Kabeyasawa and Matsumoto [151]	1764	200	200	2.130	0.800	776.0	3000	1300	80	0.530	0.530	1001.0	87.60	1062.0	134.5833	1.90
Kabeyasawa and Matsumoto [151]	1764	200	200	2.130	0.800	776.0	2000	1300	80	0.530	0.530	1001.0	93.60	1468.0	228.5714	1.49
Kabeyasawa and Matsumoto [151]	1372	200	200	2.130	0.490	713.0	3000	1300	80	0.265	0.265	753.0	55.50	717.0	235.8025	0.99
Kabeyasawa and Matsumoto [151]	1568	200	200	2.840	0.490	713.0	3000	1300	80	0.265	0.265	753.0	54.60	784.0	122.2222	0.93
Kabeyasawa and Matsumoto [151]	1372	200	200	2.840	0.490	713.0	3000	1300	80	0.530	0.530	753.0	60.30	900.0	422.2222	1.52
Kabeyasawa and Matsumoto [151]	1568	200	200	3.810	0.490	726.0	3000	1300	80	0.530	0.530	753.0	65.20	1056.0	160.6667	1.31
Luna et al. [152]	0	0	0	0.000	0.000	462.3	2867	3050	203	0.670	0.670	462.3	24.84	1125.9	331.2	1.30
Luna et al. [152]	0	0	0	0.000	0.000	434.7	1647	3050	203	1.000	1.000	434.7	48.30	2505.4	124	1.25
Luna et al. [152]	0	0	0	0.000	0.000	434.7	1647	3050	203	0.670	0.670	434.7	53.82	2082.6	61.2	2.09
Luna et al. [152]	0	0	0	0.000	0.000	462.3	1647	3050	203	0.330	0.330	462.3	28.98	1005.7	57.6	1.08
Luna et al. [152]	0	0	0	0.000	0.000	462.3	1006	3050	203	1.000	1.000	462.3	29.67	3230.7	1602	0.89
Luna et al. [152]	0	0	0	0.000	0.000	462.3	1006	3050	203	0.670	0.670	462.3	26.22	2541.0	1362.6	0.81
Luna et al. [152]	0	0	0	0.000	0.000	462.3	1006	3050	203	0.330	0.330	462.3	26.22	1415.1	2206.8	0.45
Luna et al. [152]	0	0	0	0.000	0.000	462.3	1647	3050	203	1.500	1.500	462.3	24.15	2772.4	966.6	0.70
Luna et al. [152]	0	0	0	0.000	0.000	462.3	1647	3050	203	1.500	0.670	462.3	29.67	2767.9	896.4	0.60
Luna et al. [152]	0	0	0	0.000	0.000	462.3	1647	3050	203	1.500	0.330	462.3	31.74	2202.8	945	0.52
Luna et al. [152]	0	203	395	1.500	1.500	462.3	1647	3050	203	0.670	0.670	462.3	34.50	1886.8	736.2	0.56
Luna et al. [152]	0	203	295	2.000	2.000	462.3	1647	3050	203	0.330	0.330	462.3	34.50	1624.3	693	0.89
Altin et al. [153]	0	100	100	2.000	0.150	425.0	1500	1000	100	1.830	0.150	325.0	15.50	149.0	47.6	1.05
Aaleti et al. [154]	0	150	200	5.000	0.850	413.0	6400	2300	150	0.370	0.490	413.7	35.40	840.0	28	2.00
Segura Jr and Wallace [155]	1201	330	152.4	3.180	0.920	531.0	2134	2286	152.4	0.460	0.450	578.0	35.80	419.0	124.6	2.20
Segura Jr and Wallace [155]	1201	330	152.4	3.180	1.300	531.0	2134	2286	152.4	0.460	0.450	578.0	41.70	440.0	127	2.10
Segura Jr and Wallace [155]	1201	330	152.4	3.180	0.980	531.0	2134	2286	152.4	0.460	0.450	578.0	42.40	445.0	103.8	3.00
Segura Jr and Wallace [155]	1503	330	191	3.140	1.600	531.0	2134	2286	191	0.460	0.490	578.0	46.30	583.0	189	3.00
Segura Jr and Wallace [155]	1802	330	229	3.140	1.300	531.0	2134	2286	229	0.460	0.400	578.0	48.60	703.4	184.5	3.00
Devi et al. [156]	0	100	150	1.300	1.400	400.0	3800	1000	100	0.570	0.280	400.0	30.00	157.8	16.7	2.50
Dragan et al. [157]	0	0	0	0.000	0.000	500.0	1800	880	240	1.190	1.280	500.0	40.00	382.0	100	5.00
Ganesan et al. [158]	0	100	100	1.130	1.130	415.0	700	500	60	0.570	0.180	415.0	53.00	145.0	38.5	3.60
Ganesan et al. [158]	0	100	100	1.130	1.130	415.0	700	500	60	0.570	0.180	415.0	53.00	152.0	30.8	4.00
Ganesan et al. [158]	0	130	130	1.190	1.190	415.0	2200	540	80	0.470	0.630	415.0	60.00	53.5	4.76	2.40
Ganesan et al. [158]	0	130	130	1.190	1.190	415.0	2200	540	80	0.470	0.630	415.0	60.00	55.0	5.46	2.40
Liu et al. [159]	400	100	100	8.000	0.440	4144.0	1200	700	100	0.440	0.440	4144.0	48.60	297.0	188	1.83
Liu et al. [159]	400	100	100	8.000	0.660	414.0	1200	700	100	0.660	0.660	414.0	48.60	302.0	152	1.83

Table A2. *Cont.*

Reference	A.L kN	ac mm	bc mm	ρ_{vc} %	ρ_{hc} %	Fyc MPa	hw mm	lw mm	tw mm	ρ_{vw} %	ρ_{hw} %	Fyw MPa	Fcw MPa	P kN	K kN/mm	D %
Lu et al. [160]	1200	100	200	1.170	0.180	552.0	2600	1500	200	0.330	0.330	557.0	39.10	410.3	44.5	2.50
Zhu and Guo [161]	946	200	400	2.000	0.400	438.0	3280	1700	200	0.410	0.390	451.0	35.38	682.0	38.5	2.66
Zhu and Guo [162]	1220	200	400	2.000	0.500	438.0	3400	1700	200	0.370	0.390	455.0	35.90	660.0	27	2.60
Barda et al. [163]	0	610	102	1.800	1.800	535.0	952.5	1905	102	0.500	0.500	554.0	29.40	1368.4	829.73	0.61
Barda et al. [163]	0	610	102	6.400	6.400	496.0	952.5	1905	102	0.500	0.500	562.4	16.60	1039.2	800.1	0.69
Barda et al. [163]	0	610	102	4.100	4.100	421.0	952.5	1905	102	0.500	0.500	555.3	27.40	1193.6	1100	0.56
Barda et al. [163]	0	610	102	4.100	4.100	537.0	952.5	1905	102	0.500	0.000	545.5	19.30	1097.4	1137.9	0.53
Barda et al. [163]	0	610	102	4.100	4.100	537.0	952.5	1905	102	0.000	0.500	537.0	29.40	728.9	1466.8	0.53
Barda et al. [163]	0	610	102	4.100	4.100	539.0	952.5	1905	102	0.250	0.500	506.0	21.56	929.4	1148.8	0.61
Barda et al. [163]	0	610	102	4.100	4.100	549.0	476	1905	102	0.500	0.500	541.3	26.10	1227.4	2933.7	0.85
Barda et al. [163]	0	610	102	4.100	4.100	498.0	1905	1905	102	0.500	0.500	537.7	24.15	953.8	395.1	0.56
Mansur et al. [164]	0	200	100	3.140	0.280	460.0	600	900	60	0.628	0.628	327.0	33.70	397.4	172	1.40
Mansur et al. [164]	0	200	100	3.140	0.280	460.0	600	900	60	0.550	0.550	429.0	31.40	399.6	176.2	2.50
Mansur et al. [164]	0	200	100	3.140	0.280	460.0	600	900	60	0.550	0.550	429.0	31.30	378.8	217.5	2.14
Mansur et al. [164]	0	200	100	3.140	0.280	460.0	600	900	60	0.620	0.620	359.0	37.40	414.3	241.7	2.12

Appendix B. Predictive Meta-Models

Table A3. Detailed meta-model for strength response of SPSW.

	w11	**w21**	**w31**	**w41**	**w51**	**w61**
h_f	0.66046	−0.80899	0.42823	0.01536	−0.18274	0.56987
b_f	−0.14694	−0.33524	0.10281	−0.21930	0.56121	0.07946
A_c	−0.31230	0.58567	0.50296	−0.21616	0.09030	−0.54168
I_c	−0.25301	0.09989	−0.84791	0.83422	−0.71050	−0.52802
A_b	−0.12027	−0.38129	0.00603	−0.30422	0.73080	0.34905
I_b	−0.70756	0.10070	−0.65471	−0.11693	−0.02622	1.01008
h_p	−0.11373	0.75990	−0.05930	0.37923	0.20590	−0.37343
b_p	0.87044	0.01324	−0.11518	−0.65201	0.62558	−0.58151
t_p	−0.52584	0.63379	0.89311	0.10456	−0.50542	−0.05660
F_{yp}	−0.01419	0.86811	−0.22826	0.63826	0.29556	0.20831
F_{up}	−0.40961	−0.39314	0.09353	−0.73352	0.19547	0.39709
E_p	0.27467	−0.16444	−0.48999	−0.37209	0.38294	−0.64189
	b11	b21	b31	b41	b51	b61
Bias	−1.63294	−1.18766	−0.03826	−0.16751	−0.86762	1.24930
	w12	w22	w32	w42	w52	w62
P	−0.12684	1.34651	0.45059	−0.06601	0.44606	−0.52102
	b12					
Bias	1.02066					

Table A4. Detailed meta-model for stiffness response of SPSW.

	w11	**w21**	**w31**	**w41**	**w51**	**w61**
h_f	0.37305	0.22685	0.96172	0.27180	1.48534	0.13780
b_f	−0.19722	−0.32485	−0.45253	−0.11746	−0.60365	0.88083
A_c	0.37518	0.81240	0.39296	0.71123	−0.44507	−0.83046
I_c	−0.79638	−0.29590	−0.74050	−0.30217	0.20901	0.30874
A_b	0.47524	−0.30413	−0.65031	0.63964	−0.24198	−0.63278
I_b	−0.22044	0.87375	−0.38598	0.29749	0.37306	0.22694
h_p	−0.14532	0.85001	−1.51534	−0.48506	0.02425	0.11618
b_p	0.37593	0.02488	−0.27690	0.76170	0.88023	0.90595
t_p	0.11381	0.04305	−0.37526	−0.77502	−0.92189	−0.21587
F_{yp}	0.38798	−0.53169	0.14933	0.44108	0.14424	0.79407
F_{up}	−0.79426	−0.04613	1.40176	0.68674	−0.83376	0.50377
E_p	−0.66830	0.11349	−1.27297	0.53022	−0.02661	0.05945
	b11	b21	b31	b41	b51	b61
Bias	−0.34198	−0.20046	−1.47401	−0.09315	−1.27874	0.46863
	w12	w22	w32	w42	w52	w62
k	−0.34198	−0.20046	−1.47401	−0.09315	−1.27874	0.46863
	b12					
Bias	0.80271					

Table A5. Detailed meta-model for strength response of RCSW.

	w11	**w21**	**w31**	**w41**	**w51**	**w61**	**w71**	**w81**	**w91**	**w101**
$A.L$	0.03035	0.56271	0.65166	−0.49158	0.95894	−0.25677	0.35357	1.74573	1.36929	0.07470
W_{1b}	0.00363	−0.81004	−0.28891	0.49325	−0.28890	0.97131	−0.02621	0.48072	−0.97056	0.24001
W_{2b}	0.44522	−0.27800	−0.01113	−0.94223	−0.04538	1.38581	0.34507	−1.18083	−0.18496	−0.64199
ρ_{vc}	0.44214	1.67735	0.23993	−0.18993	−0.11241	1.53625	−0.54095	−0.00594	−0.00075	−0.00729
ρ_{ch}	−0.70002	−0.62402	−0.33676	−0.88147	0.72609	−0.29662	−0.37476	1.07065	−0.31478	1.43449
F_{yc}	−0.21847	0.03408	−0.40615	0.58864	−0.25504	0.55362	−0.19680	−0.14657	−0.95686	0.22086
h_w	0.96457	0.87677	1.11667	0.39403	0.16933	0.23444	0.41240	−0.23943	0.06403	2.21632
l_w	0.75509	−0.72998	0.90047	−0.78593	3.45766	−1.78285	−2.39491	0.78037	0.99762	−1.44196
t_w	0.23458	−0.93816	0.02132	−1.07066	0.15785	−1.02085	−0.88543	−1.35955	1.16582	−0.01547
ρ_{vw}	−0.44964	0.53509	0.37030	0.44851	−2.13863	0.39363	−1.01356	−1.20354	−0.23381	−0.72274
ρ_{hw}	0.46759	0.61964	0.60364	0.60909	−0.09700	−0.04887	−0.08554	−0.07229	−0.02111	−1.10481
F_{yw}	−0.25250	−0.34851	−1.11666	0.27549	0.29564	0.62440	0.07660	1.05904	−0.28551	0.02229
f_c'	−0.63277	0.02735	0.54041	−1.64195	0.07042	0.27903	−0.17193	−0.89626	−0.00433	−0.17178
	b11	b21	b31	b41	b51	b61	b71	b81	b91	b101
Bias	1.54250	−1.05560	−0.64521	−0.27120	−0.56445	0.34340	0.67124	−0.89740	−1.64937	−1.19042
	w12	w22	w32	w42	w52	w62	w72	w82	w92	w102
P	0.80903	−1.09306	0.46271	−0.15223	−1.58711	0.42260	−1.19451	0.19695	0.20121	−0.56320
	b12									
Bias	0.27163									

Table A6. Detailed meta-model for stiffness response of RCSW.

	w11	**w21**	**w31**	**w41**	**w51**	**w61**	**w71**	**w81**	**w91**	**w101**
$A.L$	0.27836	0.34179	0.55152	0.79469	1.25982	0.90687	−0.02805	0.79850	0.09437	−0.06686
W_{1b}	−0.35504	−0.29662	0.63076	1.04187	0.28381	−1.12608	0.60906	0.77589	0.17191	−0.05209
W_{2b}	0.38845	0.06067	−0.07384	−0.10242	0.11835	0.68601	−0.51639	0.69812	−0.33039	−0.81421
ρ_{vc}	0.00685	−0.42597	−0.56353	−0.27964	0.07599	0.48414	−0.13054	0.28632	−0.56540	0.18407
ρ_{ch}	−0.18496	−0.93420	−0.21477	−1.30458	−0.25130	−0.16112	1.17348	−0.46040	−1.01113	−0.93252
F_{yc}	−0.32846	0.19449	−0.00322	−0.23876	0.00709	−0.24757	0.12753	−0.93046	0.73564	−1.19427
h_w	−2.48463	−0.53283	−0.53211	−0.16902	−1.33119	−0.02211	0.01571	−0.43720	−1.38712	1.51850
l_w	0.33724	0.90620	0.57674	0.18346	−0.22445	0.17460	−0.49526	−0.55005	0.45015	0.01144
t_w	−0.05230	0.71080	−0.49130	−0.72176	0.15461	−0.04615	0.24655	−0.73673	0.44326	−0.53894
ρ_{vw}	0.19946	1.35835	−0.56388	0.44006	−0.21862	−0.43304	−0.10659	1.16227	−0.28689	0.63142
ρ_{hw}	0.56298	0.40776	0.68201	−0.37318	−0.10458	0.18270	−0.76181	−0.20352	0.46643	0.20279
F_{yw}	0.12877	−0.02556	0.16279	0.55430	−0.10325	−0.35100	1.00406	−0.47198	0.09076	−0.07678
f_c'	−0.25932	−0.90033	0.23902	0.28550	0.11517	0.17102	−0.33770	−0.05328	0.31861	−0.72958
	b11	b21	b31	b41	b51	b61	b71	b81	b91	b101
Bias	−2.40062	−1.41379	1.54715	−0.57911	0.65255	−0.61406	−0.48502	1.07819	1.26215	4.07677
	w12	w22	w32	w42	w52	w62	w72	w82	w92	w102
K	1.22667	0.59476	−0.31743	0.59542	1.08410	−0.91750	−1.24778	−0.90334	−1.04493	−1.19961
	b12									
Bias	0.23727									

Table A7. Detailed meta-model for drift response of RCSW.

	w11	**w21**	**w31**	**w41**	**w51**	**w61**	**w71**	**w81**	**w91**	**w101**
$A.L$	−0.38551	−0.21555	0.24561	0.72432	0.22761	−0.32669	−1.22827	1.02986	0.29691	−0.65452
W_{1b}	−0.99673	0.44528	−2.90900	−0.04773	0.07769	0.14600	−0.41686	−2.04320	−0.04020	−0.30586
W_{2b}	−0.46010	0.27508	−1.58672	−0.07816	−1.17859	−0.02286	0.65862	1.95612	−0.39298	−0.07518
ρ_{vc}	0.87950	1.24468	0.58189	0.45051	−0.09522	−1.02249	−0.83121	0.20119	0.95248	−0.00905
ρ_{ch}	−0.12796	0.88787	−1.25140	−0.33128	−0.95154	−1.33210	−0.34843	1.30857	0.56996	−0.77308
F_{yc}	−0.79125	0.59283	0.61220	0.65224	−0.79856	−0.22531	0.88950	−0.53688	−0.20737	0.09254
h_w	1.01985	0.11646	0.07401	0.91305	−0.10624	−0.59715	0.53518	0.48895	−0.48217	−1.09651
l_w	−0.81903	0.56432	−0.97381	0.57371	0.29790	−1.10196	−0.38007	−0.45571	0.35466	−0.85581
t_w	0.90861	−0.48538	0.62197	0.16745	−0.22928	0.46233	0.01534	0.57427	−0.45866	0.40609
ρ_{vw}	0.14697	−0.92753	0.61884	0.57854	0.93538	−0.50672	−0.20537	−0.47842	1.45274	−0.04762
ρ_{hw}	1.19628	0.57915	0.40955	0.45958	0.11556	−0.85086	−0.68757	−0.31959	1.00650	0.12659
F_{yw}	−0.02750	1.08842	−1.35543	−0.12400	0.09936	−0.50841	0.31056	−0.21224	−0.15709	0.27799
f_c'	0.22400	−1.75419	−1.45567	−0.30999	0.52838	−0.35201	0.33484	−0.72868	0.55217	0.18422
	b11	b21	b31	b41	b51	b61	b71	b81	b91	b101
Bias	−1.62011	0.13056	−0.50546	−0.75766	−0.61882	−0.24612	0.63451	0.91834	−1.27594	−1.70098
	w12	w22	w32	w42	w52	w62	w72	w82	w92	w102
D	1.38455	−0.54226	0.41286	−0.04294	−1.17546	0.35975	−0.26591	−0.71351	−0.36289	−0.31776
	b12									
Bias	0.16445									

References

1. Bertero, V.V. The Response of Shear Walls Subjected to Dynamic Loads. Ph.D. Thesis, Massachusetts Institute of Technology, Cambridge, MA, USA, 1957.
2. Hidalgo, P.A.; Ledezma, C.A.; Jordan, R.M. Seismic behavior of squat reinforced concrete shear walls. *Earthq. Spectra* **2002**, *18*, 287–308. [CrossRef]
3. Bao, Y.; Kunnath, S.K. Simplified progressive collapse simulation of RC frame–wall structures. *Eng. Struct.* **2010**, *32*, 3153–3162. [CrossRef]
4. Kolozvari, K.; Wallace, J.W. Practical nonlinear modeling of reinforced concrete structural walls. *J. Struct. Eng.* **2016**, *142*, G4016001. [CrossRef]
5. Thorburn, L.J.; Montgomery, C.; Kulak, G.L. *Analysis of Steel Plate Shear Walls*; Technical Report; University of Alberta: Edmonton, AB, Canada, 1983.
6. Jalali, S.; Banazadeh, M. Development of a new deteriorating hysteresis model for seismic collapse assessment of thin steel plate shear walls. *Thin-Walled Struct.* **2016**, *106*, 244–257. [CrossRef]
7. Yokel, F.Y.; Fattal, S.G. Failure hypothesis for masonry shear walls. *J. Struct. Div.* **1976**, *102*, 515–532.
8. Caliò, I.; Pantò, B. A macro-element modelling approach of Infilled Frame Structures. *Comput. Struct.* **2014**, *143*, 91–107. [CrossRef]
9. Pantò, B.; Cannizzaro, F.; Caddemi, S.; Caliò, I. 3D macro-element modelling approach for seismic assessment of historical masonry churches. *Adv. Eng. Softw.* **2016**, *97*, 40–59. [CrossRef]
10. Bahmani, P.; van de Lindt, J.W. Experimental and numerical assessment of woodframe sheathing layer combinations for use in strength-based and performance-based design. *J. Struct. Eng.* **2014**, *142*, E4014001. [CrossRef]
11. Stitic, A.; Nguyen, A.C.; Rezaei Rad, A.; Weinand, Y. Numerical Simulation of the Semi-Rigid Behaviour of Integrally Attached Timber Folded Surface Structures. *Buildings* **2019**, *9*, 55. [CrossRef]
12. Timler, P.A.; Kulak, G.L. *Experimental Study of Steel Plate Shear Walls*; Technical Report; University of Alberta: Edmonton, AB, Canada, 1983.
13. Tromposch, E.W.; Kulak, G.L. *Cyclic and Static Behaviour of Thin Panel Steel Plate Shear Walls*; Technical Report; University of Alberta: Edmonton, AB, Canada, 1987.
14. Timler, P. Economical design of steel plate shear walls from a consulting engineers perspective. In *1999 North American Steel Construction Conference (NASCC)*; American Institute of Steel Construction: Chicago, IL, USA, 1999; p. 36.
15. Hajimirsadeghi, M.; Mirtaheri, M.; Zandi, A.; Hariri-Ardebili, M. Experimental cyclic test and failure modes of a full scale enhanced modular steel plate shear wall. *Eng. Fail. Anal.* **2019**, *95*, 283–288. [CrossRef]
16. AISC. *Load and Resistance Factor Design Specifications for Structural Steel Buildings*; American Institute of Steel Construction: Chicago, IL, USA, 1999.
17. CSA-S16-01. *Limit States Design of Steel Structures*; Canadian Standard Association: Toronto, ON, Canada, 2001.
18. Marzban, S.; Almasi, A.; Schwarz, J. Reinforced Concrete Structural Wall Database Development for Model Validation. In Proceedings of the 2nd European Conference on Earthquake Engineering and Seismology, Istanbul, Turkey, 25–29 August 2014.
19. Hariri-Ardebili, M.A.; Saouma, V.E. Sensitivity and uncertainty analysis of AAR affected reinforced concrete shear walls. *Eng. Struct.* **2018**, *172*, 334–345. [CrossRef]
20. Salazar, F.; Morán, R.; Toledo, M.Á.; Oñate, E. Data-based models for the prediction of dam behaviour: A review and some methodological considerations. *Arch. Comput. Methods Eng.* **2017**, *24*, 1–21. [CrossRef]
21. Hariri-Ardebili, M.A.; Pourkamali-Anaraki, F. Support vector machine based reliability analysis of concrete dams. *Soil Dyn. Earthq. Eng.* **2018**, *104*, 276–295. [CrossRef]
22. Blatman, G.; Sudret, B. Adaptive sparse polynomial chaos expansion based on least angle regression. *J. Comput. Phys.* **2011**, *230*, 2345–2367. [CrossRef]
23. Du, K.L.; Swamy, M.N. *Neural Networks in a Softcomputing Framework*; Springer Science & Business Media: London, UK, 2006.
24. McCulloch, W.S.; Pitts, W. A logical calculus of the ideas immanent in nervous activity. *Bull. Math. Biophys.* **1943**, *5*, 115–133. [CrossRef]
25. Hebb, D. *The Organization of Behavior*; Wiley: New York, NY, USA, 1949.

26. Widrow, B.; Hoff, M.E. *Adaptive Switching Circuits*; Technical Report; Stanford Univ CA Stanford Electronics Labs: Stanford, CA, USA, 1960.
27. Rosenblatt, F. *Principles of Neurodynamics. Perceptrons and the Theory of Brain Mechanisms*; Technical Report; Cornell Aeronautical Lab Inc.: Buffalo, NY, USA, 1961.
28. Rumelhart, D.E.; Hinton, G.E.; Williams, R.J. *Learning Internal Representations by Error Propagation*; Technical Report; California Univ San Diego La Jolla Inst for Cognitive Science: San Diego, CA, USA, 1985.
29. Fausett, L.V. *Fundamentals of Neural Networks: Architectures, Algorithms, and Applications*; Prentice-Hall: Englewood Cliffs, NJ, USA, 1994; Volume 3.
30. Cybenko, G. Approximation by superpositions of a sigmoidal function. *Math. Control Signals Syst.* **1989**, *2*, 303–314. [CrossRef]
31. Funahashi, K.I. On the approximate realization of continuous mappings by neural networks. *Neural Netw.* **1989**, *2*, 183–192. [CrossRef]
32. Hornik, K.; Stinchcombe, M.; White, H. Multilayer feedforward networks are universal approximators. *Neural Netw.* **1989**, *2*, 359–366. [CrossRef]
33. Xiang, C.; Ding, S.Q.; Lee, T.H. Geometrical interpretation and architecture selection of MLP. *IEEE Trans. Neural Netw.* **2005**, *16*, 84–96. [CrossRef]
34. Cybenko, G. *Continuous Valued Neural Networks with Two Hidden Layers Are Sufficient*; Technical Report; Department of Computer Science, Tufts University: Medford, MA, USA, 1988.
35. Bui, T.Q.; Tran, A.V.; Shah, A.A. Improved knowledge-based neural network (KBNN) model for predicting spring-back angles in metal sheet bending. *Int. J. Model. Simul. Sci. Comput.* **2014**, *5*, 1350026. [CrossRef]
36. Chester, D.L. *Why Two Hidden Layers Are Better than One*; Proc. IJCNN: Washington, DC, USA, 1990; Volume 1, pp. 265–268.
37. Adeli, H.; Seon Park, H. Counterpropagation neural networks in structural engineering. *J. Struct. Eng.* **1995**, *121*, 1205–1212. [CrossRef]
38. Xu, Y.; Liu, G.; Wu, Z.; Huang, X. Adaptive multilayer perceptron networks for detection of cracks in anisotropic laminated plates. *Int. J. Solids Struct.* **2001**, *38*, 5625–5645. [CrossRef]
39. De Lima, L.; Vellasco, P.D.S.; De Andrade, S.; Da Silva, J.; Vellasco, M. Neural networks assessment of beam-to-column joints. *J. Braz. Soc. Mech. Sci. Eng.* **2005**, *27*, 314–324. [CrossRef]
40. Abdalla, J.A.; Elsanosi, A.; Abdelwahab, A. Modeling and simulation of shear resistance of R/C beams using artificial neural network. *J. Frankl. Inst.* **2007**, *344*, 741–756. [CrossRef]
41. Kumar, R.; Mishra, B.; Jain, S. Vibration control of smart composite laminated spherical shell using neural network. *J. Intell. Mater. Syst. Struct.* **2008**, *19*, 947–957. [CrossRef]
42. González, M.P.; Zapico, J.L. Seismic damage identification in buildings using neural networks and modal data. *Comput. Struct.* **2008**, *86*, 416–426. [CrossRef]
43. Yan, B.; Cui, Y.; Zhang, L.; Zhang, C.; Yang, Y.; Bao, Z.; Ning, G. Beam structure damage identification based on BP neural network and support vector machine. *Math. Probl. Eng.* **2014**, *2014*, 850141. [CrossRef]
44. Lee, S.; Lee, C. Prediction of shear strength of FRP-reinforced concrete flexural members without stirrups using artificial neural networks. *Eng. Struct.* **2014**, *61*, 99–112. [CrossRef]
45. Asteris, P.G.; Plevris, V. Anisotropic masonry failure criterion using artificial neural networks. *Neural Comput. Appl.* **2017**, *28*, 2207–2229. [CrossRef]
46. Toghroli, A.; Suhatril, M.; Ibrahim, Z.; Safa, M.; Shariati, M.; Shamshirband, S. Potential of soft computing approach for evaluating the factors affecting the capacity of steel–concrete composite beam. *J. Intell. Manuf.* **2018**, *29*, 1793–1801. [CrossRef]
47. Naderpour, H.; Poursaeidi, O.; Ahmadi, M. Shear resistance prediction of concrete beams reinforced by FRP bars using artificial neural networks. *Measurement* **2018**, *126*, 299–308. [CrossRef]
48. Rezaei Rad, A.; Banazadeh, M. Probabilistic risk-based performance evaluation of seismically base-isolated steel structures subjected to far-field earthquakes. *Buildings* **2018**, *8*, 128. [CrossRef]
49. Ghorbani, A.; Hasanzadehshooiili, H.; Sadowski, Ł. Neural Prediction of Tunnels' Support Pressure in Elasto-Plastic, Strain-Softening Rock Mass. *Appl. Sci.* **2018**, *8*, 841. [CrossRef]
50. Asteris, P.G.; Kolovos, K.G. Self-compacting concrete strength prediction using surrogate models. *Neural Comput. Appl.* **2019**, *31*, 409–424. [CrossRef]
51. Chen, H.; Asteris, P.G.; Jahed Armaghani, D.; Gordan, B.; Pham, B.T. Assessing Dynamic Conditions of the Retaining Wall: Developing Two Hybrid Intelligent Models. *Appl. Sci.* **2019**, *9*, 1042. [CrossRef]

52. Asteris, P.G.; Nikoo, M. Artificial bee colony-based neural network for the prediction of the fundamental period of infilled frame structures. *Neural Comput. Appl.* **2019**, 1–11. [CrossRef]
53. Li, H.; Chen, C.P.; Huang, H.P. *Fuzzy Neural Intelligent Systems: Mathematical Foundation and the Applications in Engineering*; CRC Press: Boca Raton, FL, USA, 2000.
54. Thimm, G.; Fiesler, E. High-order and multilayer perceptron initialization. *IEEE Trans. Neural Netw.* **1997**, *8*, 349–359. [CrossRef]
55. Hirose, Y.; Yamashita, K.; Hijiya, S. Back-propagation algorithm which varies the number of hidden units. *Neural Netw.* **1991**, *4*, 61–66. [CrossRef]
56. Ozturan, M.; Kutlu, B.; Ozturan, T. Comparison of concrete strength prediction techniques with artificial neural network approach. *Build. Res. J.* **2008**, *56*, 23–36.
57. Hecht-Nielsen, R. Kolmogorov's mapping neural network existence theorem. In *Proceedings of the International Conference on Neural Networks*; IEEE Press: New York, NY, USA, 1987; Volume 3, pp. 11–14.
58. Hush, D.R. Classification with neural networks: A performance analysis. In Proceedings of the IEEE International Conference on Systems Engineering, Fairborn, OH, USA, 24–26 August 1989; pp. 277–280.
59. Ripley, B.D. Statistical aspects of neural networks. *Netw. Chaos Stat. Probab. Asp.* **1993**, *50*, 40–123.
60. Gallant, S.I.; Gallant, S.I. *Neural Network Learning and Expert Systems*; MIT Press: Cambridge, MA, USA, 1993.
61. Wang, C. A Theory of Generalization in Learning Machines with Neural Network Applications. Ph.D. Thesis, University of Pennsylvania, Philadelphia, PA, USA, 1994.
62. Masters, T. *Practical Neural Network Recipes in C++*; Morgan Kaufmann: Burlington, MA, USA, 1993.
63. Paola, J. Neural Network Classification of Multispectral Imagery. Master's Thesis, The University of Arizona, Tucson, AZ, USA, 1994.
64. Li, J.Y.; Chow, T.W.; Yu, Y.L. The estimation theory and optimization algorithm for the number of hidden units in the higher-order feedforward neural network. In Proceedings of the ICNN'95-International Conference on Neural Networks, Perth, WA, Australia, 27 November–1 December 1995; Volume 3, pp. 1229–1233.
65. Tamura, S.; Tateishi, M. Capabilities of a four-layered feedforward neural network: four layers versus three. *IEEE Trans. Neural Netw.* **1997**, *8*, 251–255. [CrossRef] [PubMed]
66. Lai, S.; Serra, M. Concrete strength prediction by means of neural network. *Constr. Build. Mater.* **1997**, *11*, 93–98. [CrossRef]
67. Nagendra, S. *Practical Aspects of Using Neural Networks: Necessary Preliminary Specifications*; Technical Paper; GE Research and Development Center: Niskayuna, NY, USA, 1998.
68. Gencay, R. Linear, non-linear and essential foreign exchange rate prediction with simple technical trading rules. *J. Int. Econ.* **1999**, *47*, 91–107. [CrossRef]
69. Chris Wong, C.C.; Chan, M.C.; Lam, C.C. Financial Time Series Forecasting By Neural Network Using Conjugate Gradient Learning Algorithm And Multiple Linear Regression Weight Initialization. *Soc. Comput. Econ. Comput. Econ. Financ.* **2000**, *61*, 326–342.
70. Heaton, J. *Artificial Intelligence for Humans. Volume 1: Fundamental Algorithms*; CreateSpace Independent Publishing: North Charleston, SC, USA, 2013.
71. Zhang, Z.; Ma, X.; Yang, Y. Bounds on the number of hidden neurons in three-layer binary neural networks. *Neural Netw.* **2003**, *16*, 995–1002. [CrossRef]
72. Huang, G.B. Learning capability and storage capacity of two-hidden-layer feedforward networks. *IEEE Trans. Neural Netw.* **2003**, *14*, 274–281. [CrossRef] [PubMed]
73. Ke, J.; Liu, X. Empirical analysis of optimal hidden neurons in neural network modeling for stock prediction. In Proceedings of the 2008 IEEE Pacific-Asia Workshop on Computational Intelligence and Industrial Application, Wuhan, China, 19–20 December 2008; Volume 2, pp. 828–832.
74. Trenn, S. Multilayer perceptrons: Approximation order and necessary number of hidden units. *IEEE Trans. Neural Netw.* **2008**, *19*, 836–844. [CrossRef] [PubMed]
75. Shibata, K.; Ikeda, Y. Effect of number of hidden neurons on learning in large-scale layered neural networks. In Proceedings of the 2009 ICCAS-SICE, Fukuoka, Japan, 18–21 August 2009; pp. 5008–5013.
76. Hunter, D.; Yu, H.; Pukish, M.; Kolbusz, J.; Wilamowski, B. Selection of Proper Neural Network Sizes and Architectures—A Comparative Study. *IEEE Trans. Ind. Inform.* **2012**, *8*, 228–240. [CrossRef]
77. Sheela, K.G.; Deepa, S.N. Review on methods to fix number of hidden neurons in neural networks. *Math. Probl. Eng.* **2013**, *2013*, 425740. [CrossRef]
78. Garson, G. Interpreting Neural-Network Connection Strengths. *AI Expert* **1991**, *6*, 47–51.

79. Goh, A. Back-Propagation Neural Networks for Modeling Complex Systems. *Artif. Intell. Eng.* **1995**, *9*, 143–151. [CrossRef]
80. Behbahanifard, M.R.; Grondin, G.Y.; Elwi, A.E.A. *Experimental and Numerical Investigation of Steel Plate Shear Walls*; Department of Civil and Environmental Engineering, University of Alberta: Edmonton, AB, Canada, 2003.
81. Sigariyazd, M.A.; Joghataie, A.; Attari, N.K. Analysis and design recommendations for diagonally stiffened steel plate shear walls. *Thin-Walled Struct.* **2016**, *103*, 72–80. [CrossRef]
82. Shekastehband, B.; Azaraxsh, A.; Showkati, H.; Pavir, A. Behavior of semi-supported steel shear walls: Experimental and numerical simulations. *Eng. Struct.* **2017**, *135*, 161–176. [CrossRef]
83. Berman, J.W.; Celik, O.C.; Bruneau, M. Comparing hysteretic behavior of light-gauge steel plate shear walls and braced frames. *Eng. Struct.* **2005**, *27*, 475–485. [CrossRef]
84. Yu, J.G.; Feng, X.T.; Li, B.; Hao, J.P. Cyclic performance of cross restrained steel plate shear walls with transverse braces. *Thin-Walled Struct.* **2018**, *132*, 250–264. [CrossRef]
85. Choi, I.R.; Park, H.G. Ductility and energy dissipation capacity of shear-dominated steel plate walls. *J. Struct. Eng.* **2008**, *134*, 1495–1507. [CrossRef]
86. Wang, M.; Shi, Y.; Xu, J.; Yang, W.; Li, Y. Experimental and numerical study of unstiffened steel plate shear wall structures. *J. Constr. Steel Res.* **2015**, *112*, 373–386. [CrossRef]
87. Sabouri-Ghomi, S.; Sajjadi, S.R.A. Experimental and theoretical studies of steel shear walls with and without stiffeners. *J. Constr. Steel Res.* **2012**, *75*, 152–159. [CrossRef]
88. Chen, S.J.; Jhang, C. Experimental study of low-yield-point steel plate shear wall under in-plane load. *J. Constr. Steel Res.* **2011**, *67*, 977–985. [CrossRef]
89. Nateghi-Alahi, F.; Khazaei-Poul, M. Experimental study of steel plate shear walls with infill plates strengthened by GFRP laminates. *J. Constr. Steel Res.* **2012**, *78*, 159–172. [CrossRef]
90. Caccese, V.; Elgaaly, M.; Chen, R. Experimental study of thin steel-plate shear walls under cyclic load. *J. Struct. Eng.* **1993**, *119*, 573–587. [CrossRef]
91. Alavi, E.; Nateghi, F. Experimental study on diagonally stiffened steel plate shear walls with central perforation. *J. Constr. Steel Res.* **2013**, *89*, 9–20. [CrossRef]
92. Park, H.G.; Kwack, J.H.; Jeon, S.W.; Kim, W.K.; Choi, I.R. Framed steel plate wall behavior under cyclic lateral loading. *J. Struct. Eng.* **2007**, *133*, 378–388. [CrossRef]
93. Lubell, A.S.; Prion, H.G.; Ventura, C.E.; Rezai, M. Unstiffened steel plate shear wall performance under cyclic loading. *J. Struct. Eng.* **2000**, *126*, 453–460. [CrossRef]
94. Roberts, T.M.; Sabouri-Ghomi, S. Hysteretic characteristics of unstiffened perforated steel plate shear panels. *Thin-Walled Struct.* **1992**, *14*, 139–151. [CrossRef]
95. Carrillo, J.; Lizarazo, J.M.; Bonett, R. Effect of lightweight and low-strength concrete on seismic performance of thin lightly-reinforced shear walls. *Eng. Struct.* **2015**, *93*, 61–69. [CrossRef]
96. Yuan, W.; Zhao, J.; Sun, Y.; Zeng, L. Experimental study on seismic behavior of concrete walls reinforced by PC strands. *Eng. Struct.* **2018**, *175*, 577–590. [CrossRef]
97. Shiga, T.; Shibata, A.; Takahashi, J. Experimental study on dynamic properties of reinforced concrete shear walls. In Proceedings of the Fifth World Conference on Earthquake Engineering, Rome, Italy, 25–29 June 1973; Volume 1, pp. 1157–1166.
98. Greifenhagen, C.; Lestuzzi, P. Static cyclic tests on lightly reinforced concrete shear walls. *Eng. Struct.* **2005**, *27*, 1703–1712. [CrossRef]
99. Looi, D.; Su, R.; Cheng, B.; Tsang, H. Effects of axial load on seismic performance of reinforced concrete walls with short shear span. *Eng. Struct.* **2017**, *151*, 312–326. [CrossRef]
100. Lopes, M. Experimental shear-dominated response of RC walls. Part II: Discussion of results and design implications. *Eng. Struct.* **2001**, *23*, 564–574. [CrossRef]
101. Yanez, F.; Park, R.; Paulay, T. Seismic behaviour of reinforced concrete structural walls with irregular openings. In Proceedings of the Pacific Conference on Earthquake Engineering, Auckland, New Zealand, 20–23 November 1991; pp. 3303–3308.
102. Bouchon, M.; Orbovic, N.; Foure, N. Tests on reinforced concrete low-rise shear walls under static cyclic loading. In Proceedings of the 13th World Conference on Earthquake Engineering, Vancouver, BC, Canada, 1–6 August 2004; p. 10.
103. Tasnimi, A. Strength and deformation of mid-rise shear walls under load reversal. *Eng. Struct.* **2000**, *22*, 311–322. [CrossRef]

104. Lefas, I.D.; Kotsovos, M.D.; Ambraseys, N.N. Behavior of reinforced concrete structural walls: Strength, deformation characteristics, and failure mechanism. *Struct. J.* **1990**, *87*, 23–31.
105. Lefas, I.D.; Kotsovos, M.D. Strength and deformation characteristics of reinforced concrete walls under load reversals. *Struct. J.* **1990**, *87*, 716–726.
106. Pilakoutas, K.; Elnashai, A. Cyclic behavior of reinforced concrete cantilever walls, Part I: Experimental results. *ACI Struct. J.* **1995**, *92*, 271–281.
107. Gupta, A.; Rangan, B.V. High-strength concrete (HSC) structural walls. *Struct. J.* **1998**, *95*, 194–204.
108. Mickleborough, N.C.; Ning, F.; Chan, C.M. Prediction of stiffness of reinforced concrete shearwalls under service loads. *Struct. J.* **1999**, *96*, 1018–1026.
109. Sittipunt, C.; Wood, S.L.; Lukkunaprasit, P.; Pattararattanakul, P. Cyclic behavior of reinforced concrete structural walls with diagonal web reinforcement. *Struct. J.* **2001**, *98*, 554–562.
110. Zhang, Y.; Wang, Z. Seismic behavior of reinforced concrete shear walls subjected to high axial loading. *Struct. J.* **2000**, *97*, 739–750.
111. Adebar, P.; Ibrahim, A.M.; Bryson, M. Test of high-rise core wall: Effective stiffness for seismic analysis. *ACI Struct. J.* **2007**, *104*, 549.
112. Terzioglu, T.; Orakcal, K.; Massone, L.M. Cyclic lateral load behavior of squat reinforced concrete walls. *Eng. Struct.* **2018**, *160*, 147–160. [CrossRef]
113. Abdulridha, A.; Palermo, D. Behaviour and modelling of hybrid SMA-steel reinforced concrete slender shear wall. *Eng. Struct.* **2017**, *147*, 77–89. [CrossRef]
114. Qazi, S.; Michel, L.; Ferrier, E. Seismic behaviour of RC short shear wall strengthened with externally bonded CFRP strips. *Compos. Struct.* **2019**, *211*, 390–400. [CrossRef]
115. Christidis, K.I.; Trezos, K.G. Experimental investigation of existing non-conforming RC shear walls. *Eng. Struct.* **2017**, *140*, 26–38. [CrossRef]
116. Wang, W.; Wang, Y.; Lu, Z. Experimental study on seismic behavior of steel plate reinforced concrete composite shear wall. *Eng. Struct.* **2018**, *160*, 281–292. [CrossRef]
117. Ren, F.; Chen, J.; Chen, G.; Guo, Y.; Jiang, T. Seismic behavior of composite shear walls incorporating concrete-filled steel and FRP tubes as boundary elements. *Eng. Struct.* **2018**, *168*, 405–419. [CrossRef]
118. Le Nguyen, K.; Brun, M.; Limam, A.; Ferrier, E.; Michel, L. Pushover experiment and numerical analyses on CFRP-retrofit concrete shear walls with different aspect ratios. *Compos. Struct.* **2014**, *113*, 403–418. [CrossRef]
119. Choi, C.S. Improvement of earthquake-resistant performance of squat shear walls under reversed cyclic loads. *Key Eng. Mater.* **2006**, *324*, 535–538. [CrossRef]
120. Cortés-Puentes, W.L.; Palermo, D. Performance of pre-1970s squat reinforced concrete shear walls. *Can. J. Civ. Eng.* **2018**, *45*, 922–935. [CrossRef]
121. Cortés-Puentes, W.L.; Palermo, D. Seismic retrofit of concrete shear walls with SMA tension braces. *J. Struct. Eng.* **2017**, *144*, 04017200. [CrossRef]
122. Cortés-Puentes, W.L.; Palermo, D. Modeling of RC shear walls retrofitted with steel plates or FRP sheets. *J. Struct. Eng.* **2011**, *138*, 602–612. [CrossRef]
123. Qiao, Q.; Cao, W.; Qian, Z.; Li, X.; Zhang, W.; Liu, W. Cyclic behavior of low rise concrete shear walls containing recycled coarse and fine aggregates. *Materials* **2017**, *10*, 1400. [CrossRef] [PubMed]
124. Blandon, C.A.; Arteta, C.A.; Bonett, R.L.; Carrillo, J.; Beyer, K.; Almeida, J.P. Response of thin lightly-reinforced concrete walls under cyclic loading. *Eng. Struct.* **2018**, *176*, 175–187. [CrossRef]
125. Christidis, K.I.; Vougioukas, E.; Trezos, K.G. Strengthening of non-conforming RC shear walls using different steel configurations. *Eng. Struct.* **2016**, *124*, 258–268. [CrossRef]
126. Liao, F.Y.; Han, L.H.; Tao, Z. Performance of reinforced concrete shear walls with steel reinforced concrete boundary columns. *Eng. Struct.* **2012**, *44*, 186–209. [CrossRef]
127. Dazio, A.; Beyer, K.; Bachmann, H. Quasi-static cyclic tests and plastic hinge analysis of RC structural walls. *Eng. Struct.* **2009**, *31*, 1556–1571. [CrossRef]
128. Zhi, Q.; Guo, Z.; Xiao, Q.; Yuan, F.; Song, J. Quasi-static test and strut-and-tie modeling of precast concrete shear walls with grouted lap-spliced connections. *Constr. Build. Mater.* **2017**, *150*, 190–203. [CrossRef]
129. Shen, D.; Yang, Q.; Jiao, Y.; Cui, Z.; Zhang, J. Experimental investigations on reinforced concrete shear walls strengthened with basalt fiber-reinforced polymers under cyclic load. *Constr. Build. Mater.* **2017**, *136*, 217–229. [CrossRef]

130. Zhang, J.W.; Zheng, W.B.; Cao, W.L.; Dong, H.Y.; Li, W.D. Seismic Behavior of Low-rise Concrete Shear Wall with Single Layer of Web Reinforcement and Inclined Rebars: Restoring Force Model. *KSCE J. Civ. Eng.* **2019**, *23*, 1302–1319. [CrossRef]
131. Ji, X.; Cheng, X.; Xu, M. Coupled axial tension-shear behavior of reinforced concrete walls. *Eng. Struct.* **2018**, *167*, 132–142. [CrossRef]
132. Mohamed, N.; Farghaly, A.S.; Benmokrane, B.; Neale, K.W. Numerical simulation of mid-rise concrete shear walls reinforced with GFRP bars subjected to lateral displacement reversals. *Eng. Struct.* **2014**, *73*, 62–71. [CrossRef]
133. Quiroz, L.G.; Maruyama, Y.; Zavala, C. Cyclic behavior of thin RC Peruvian shear walls: Full-scale experimental investigation and numerical simulation. *Eng. Struct.* **2013**, *52*, 153–167. [CrossRef]
134. Salonikios, T.; Kappos, A.; Tegos, I.A.; Penelis, G. Cyclic Load Behavior of Low-slenderness R/C Walls: Design Basis and Test Results. *ACI Struct. J.* **1999**, *4*, 649–660.
135. Thomsen, J.H. Displacement Based Design of Reinforced Concrete Structural Walls: An Experimental Investigation of Walls with Rectangular and t-Shaped Cross-Sections: A Dissertation. Ph.D. Thesis, Clarkson University Richmond, Ontario County, NY, USA, 1995.
136. Tran, T.A.; Wallace, J. Experimental study of nonlinear flexural and shear deformations of reinforced concrete structural walls. In Proceedings of the 15th World Conference on Earthquake Engineering, Lisbon, Portugal, 24–28 September 2012.
137. Layssi, H.; Mitchell, D. Experiments on seismic retrofit and repair of reinforced concrete shear walls. In Proceedings of the 6th International Conference on FRP Composites in Civil Engineering (CICE), Rome, Italy, 13–15 June 2012; pp. 13–15.
138. Ghorbani-Renani, I.; Velev, N.; Tremblay, R.; Palermo, D.; Massicotte, B.; Léger, P. Modeling and Testing Influence of Scaling Effects on Inelastic Response of Shear Walls. *ACI Struct. J.* **2009**, *106*, 358–367.
139. Ghazizadeh, S.; Cruz-Noguez, C.A.; Li, Y. Numerical study of hybrid GFRP-steel reinforced concrete shear walls and SFRC walls. *Eng. Struct.* **2019**, *180*, 700–712. [CrossRef]
140. Ghazizadeh, S.; Cruz-Noguez, C.A. Damage-resistant reinforced concrete low-rise walls with hybrid GFRP-steel reinforcement and steel fibers. *J. Compos. Constr.* **2018**, *22*, 04018002. [CrossRef]
141. Athanasopoulou, A. Shear Strength and Drift Capacity of Reinforced Concrete and High-Performance Fiber Reinforced Concrete Low-Rise Walls Subjected to Displacement Reversals. Ph.D. Thesis, University of Michigan, Ann Arbor, MI, USA, 2010.
142. Tupper, B. Seismic Response of Reinforced Concrete Walls with Steel Boundary Elements. Ph.D. Thesis, McGill University Libraries, Montreal, QC, Canada, 1999.
143. Arafa, A.; Farghaly, A.; Benmokrane, B. Effect of web reinforcement on the seismic response of concrete squat walls reinforced with glass-FRP bars. *Eng. Struct.* **2018**, *174*, 712–723. [CrossRef]
144. Oesterle, R.G.; Fiorato, A.E.; Aristizabal-Ochoa, J.D.; Corley, W.G. Hysteretic Response of Reinforced Concrete Structural Walls. *ACI Spec. Publ. SP63-11* **1980**, *63*, 243–273.
145. Oesterle, R.; Fiorato, A.; Corley, W. Reinforcement details for earthquake-resistant structural walls. *Concr. Int.* **1980**, *2*, 55–66.
146. Shiu, K.; Daniel, J.; Aristizabal-Ochoa, J.; Fiorato, A.; Corley, W. *Earthquake Resistant Structural Walls: Test of Walls With and Without Openings*; NASA STI/Recon Technical Report N; NASA: Boston, MA, USA, 1981; Volume 82.
147. Jiang, H.J.; Lu, X.L. Calculating Method for the Hysteretic Characteristics of Shear Walls Dissipating Energy along the Vertical Direction. *J. Tongji Univ.* **1999**, *6*. [CrossRef]
148. Park, H.G.; Baek, J.W.; Lee, J.H.; Shin, H.M. Cyclic Loading Tests for Shear Strength of Low-Rise Reinforced Concrete Walls with Grade 550 MPa Bars. *ACI Struct. J.* **2015**, *112*, 299–310. [CrossRef]
149. Hube, M.; Santa María, H.; López, M. Experimental Campaign of thin Reinforced Concrete Shear Walls for Low-Rise Constructions. In Proceedings of the 16th World Conference on Earthquake Engineering, Santiago, Chile, 9–13 January 2017.
150. Alarcon, C.; Hube, M.; De la Llera, J. Effect of axial loads in the seismic behavior of reinforced concrete walls with unconfined wall boundaries. *Eng. Struct.* **2014**, *73*, 13–23. [CrossRef]
151. Kabeyasawa, T.; Matsumoto, K. Tests and analyses of ultra-high strength reinforced concrete shear walls. In Proceedings of the 10th World Conference on Earthquake Engineering, Madrid, Spain, 19–24 July 1992; pp. 3291–3296.

152. Luna, B.N.; Rivera, J.P.; Whittaker, A.S. Seismic behavior of low-aspect-ratio reinforced concrete shear walls. *ACI Struct. J.* **2015**, *112*, 593. [CrossRef]
153. Altin, S.; Anil, Ö.; Kopraman, Y.; Kara, M.E. Hysteretic behavior of RC shear walls strengthened with CFRP strips. *Compos. Part B Eng.* **2013**, *44*, 321–329. [CrossRef]
154. Aaleti, S.; Brueggen, B.L.; Johnson, B.; French, C.E.; Sritharan, S. Cyclic response of reinforced concrete walls with different anchorage details: Experimental investigation. *J. Struct. Eng.* **2012**, *139*, 1181–1191. [CrossRef]
155. Segura, C.L., Jr.; Wallace, J.W. Seismic Performance Limitations and Detailing of Slender Reinforced Concrete Walls. *ACI Struct. J.* **2018**, *115*, 849–859. [CrossRef]
156. Devi, G.; Subramanian, K.; Santhakumar, A. Experimental investigations on reinforced concrete lateral load resisting systems under lateral loads. *Exp. Tech.* **2011**, *35*, 59–73. [CrossRef]
157. Dragan, D.; Plumier, A.; Degée, H. Experimental Study Regarding Shear Behavior of Concrete Walls Reinforced by Multiple Steel Profiles. In *High Tech Concrete: Where Technology and Engineering Meet*; Springer: Berlin/Heidelberg, Germany, 2018; pp. 1077–1084.
158. Ganesan, N.; Indira, P.; Seena, P. Reverse Cyclic Tests on High Performance Cement Concrete Shear Walls with Barbells. In *Advances in Structural Engineering*; Springer: Berlin/Heidelberg, Germany, 2015; pp. 2309–2321.
159. Liu, G.R.; Song, Y.P.; Qu, F.L. Post-fire cyclic behavior of reinforced concrete shear walls. *J. Cent. South Univ. Technol.* **2010**, *17*, 1103–1108. [CrossRef]
160. Lu, X.; Wang, D.; Zhao, B. Experimental Study on Seismic Performance of Precast Concrete Shear Wall with Joint Connecting Beam Under Cyclic Loadings. In *Experimental Research in Earthquake Engineering*; Springer: Berlin/Heidelberg, Germany, 2015; pp. 373–386.
161. Zhu, Z.; Guo, Z. Experimental study on emulative hybrid precast concrete shear walls. *KSCE J. Civil Eng.* **2017**, *21*, 329–338. [CrossRef]
162. Zhu, Z.; Guo, Z. Seismic Behavior of Precast Concrete Shear Walls with Different Confined Boundary Elements. *KSCE J. Civil Eng.* **2019**, *23*, 711–718. [CrossRef]
163. Barda, F.; Hanson, J.M.; Corley, W.G. Shear strength of low-rise walls with boundary elements. *Spec. Publ.* **1977**, *53*, 149–202.
164. Mansur, M.; Balendra, T.; H'ng, S. Tests on reinforced concrete low-rise shear walls under cyclic loading. In *Concrete Shear in Earthquake*; CRC Press: Boca Raton, FL, USA, 1992; pp. 14–16.